AJRCCM Articles in Press. Published on 29-October-2019 as 10.1164/rccm.201906-1141OC

Characterization of *GDF2* Mutations and Levels of BMP9 and BMP10 in Pulmonary Arterial Hypertension

Joshua Hodgson[1] • Emilia M. Swietlik[1,5] • Richard M. Salmon[1] • Charaka Hadinnapola[1] • Ivana Nikolic[26] • John Wharton[9] • Jingxu Guo[1] • James Liley[1] • Matthias Haimel[1,2,3] • Marta Bleda[1] • Laura Southgate[14,15] • Rajiv D. Machado[15] • Jennifer M. Martin[1,2,3] • Carmen M. Treacy[1,5] • Katherine Yates[1,2,3] • Louise C. Daugherty[2,3] • Olga Shamardina[2,3] • Deborah Whitehorn[2,3] • Simon Holden[4] • Harm J. Bogaard[19] • Colin Church[16] • Gerry Coghlan[11] • Robin Condliffe[7] • Paul A. Corris[6] • Cesare Danesino[24,21] • Mélanie Eyries[19] • Henning Gall[22] • Stefano Ghio[21] • Hossein-Ardeschir Ghofrani[22,9] • J. Simon R. Gibbs[10] • Barbara Girerd[20] • Arjan C. Houweling[18] • Luke Howard[9] • Marc Humbert[20] • David G. Kiely[7] • Gabor Kovacs[23,25] • Allan Lawrie[8] • Robert V. MacKenzie Ross[17] • Shahin Moledina[12] • David Montani[20] • Andrea Olschewski[23] • Horst Olschewski[23,25] • Willem H. Ouwehand[2,3] • Andrew J. Peacock[16] • Joanna Pepke-Zaba[5] • Inga Prokopenko[9] • Christopher J. Rhodes[9] • Laura Scelsi[21] • Werner Seeger[22] • Florent Soubrier[19] • Jay Suntharalingam[17] • Mark R. Toshner[1,5] • Richard C. Trembath[14] • Anton Vonk Noordegraaf[18] • Stephen J. Wort[10,13] • Martin R. Wilkins[9] • Paul B. Yu[26] • Wei Li[1] • Stefan Gräf[1,2,3] • Paul D. Upton[*1] • Nicholas W. Morrell[*1,3] * Joint senior authors

1 Department of Medicine, University of Cambridge, Cambridge CB2 0QQ United Kingdom 2 Department of Haematology, University of Cambridge, Cambridge CB2 0PT United Kingdom 3 NIHR BioResource - Rare Diseases Cambridge, CB2 0PT United Kingdom 4 Addenbrooke's Hospital, Cambridge CB2 0QQ United Kingdom 5 Royal Papworth Hospital, Papworth CB23 3RE United Kingdom 6 University of Newcastle, Newcastle NE1 7RU United Kingdom 7 Sheffield Pulmonary Vascular Disease Unit, Royal Hallamshire Hospital, Sheffield S10 2JF United Kingdom 8 Department of Infection, Immunity & Cardiovascular

Disease, University of Sheffield, Sheffield S10 2RX United Kingdom 9 Department of Medicine, Imperial College London, London W12 0NN, United Kingdom 10 National Heart & Lung Institute, Imperial College London, London SW3 6LY United Kingdom 11 Royal Free Hospital, London NW3 2QG United Kingdom 12 Great Ormond Street Hospital, London WC1N 3JH United Kingdom 13 Royal Brompton Hospital, London SW3 6NP United Kingdom 14 Department of Medical & Molecular Genetics, King's College London, London SE1 9RT United Kingdom 15 Molecular and Clinical Sciences Research Institute, St George's University of London, London SW17 0RE United Kingdom 16 Golden Jubilee National Hospital, Glasgow G81 4DY United Kingdom 17 Royal United Hospitals Bath NHS Foundation Trust, Bath BA1 3NG United Kingdom 18 Department of Clinical Genetics, Amsterdam UMC, Vrije Universiteit Amsterdam, Amsterdam, The Netherlands 19 Département de génétique, hôpital Pitié-Salpêtrière, Assistance Publique-Hôpitaux de Paris, and UMR_S 1166-ICAN, INSERM, UPMC Sorbonne Universités, Paris 75252 France 20 Université Paris-Sud, Faculté de Médecine, Université Paris-Saclay; AP-HP, Service de Pneumologie, Centre de référence de l'hypertension pulmonaire; INSERM UMR_S 999, Hôpital Bicêtre, Le Kremlin-Bicêtre, Paris 94270 France 21 Fondazione IRCCS Policlinico San Matteo, Pavia 27100 Italy 22 University of Giessen and Marburg Lung Center (UGMLC), member of the German Center for Lung Research (DZL) and of the Excellence Cluster Cardio-Pulmonary Institute (CPI), Giessen 35392 Germany 23 Ludwig Boltzmann Institute for Lung Vascular Research, Graz 8010 Austria 24 Department of Molecular Medicine, University of Pavia, Pavia 27100 Italy 25 Medical University of Graz, Graz 8036 Austria 26 Department of Medicine, Brigham and Women's Hospital and Harvard Medical School, Boston MA 02115 United States.

AJRCCM Articles in Press. Published on 29-October-2019 as 10.1164/rccm.201906-1141OC

Corresponding Authors

Professor Nicholas W. Morrell, M.D., Department of Medicine, University of Cambridge, Level 5 Addenbrooke's Hospital, Box 157, Hills Road, Cambridge, CB2 0QQ United Kingdom • nwm23@cam.ac.uk • (+44) 1223 331666

Doctor Paul Upton, Ph.D., Department of Medicine, University of Cambridge, Level 5 Addenbrooke's Hospital, Box 157, Hills Road, Cambridge, CB2 0QQ United Kingdom • pdu21@medschl.cam.ac.uk • (+44) 1223 761304

Author Contributions

All authors collected data and provided constructive criticism of the study manuscript. JH, EMS, RMS, JG, CH, WL, SG, PDU and NWM undertook the study design and interpretation. JH, EMS, JL, CH, SG and PDU analysed data.

Funding

National Institute for Health Research, British Heart Foundation, Medical Research Council, Wellcome Trust, Dinosaur Trust, Great Ormond Street Hospital Charity, Assistance Publique-Hôpitaux de Paris, Inserm, Université Paris-Sud, and Agence Nationale de la Recherche.

Running title: BMP9 and BMP10 in PAH

Subject descriptor: 17.6 Pulmonary Hypertension: Experimental

Short summary: This manuscript provides new genetic evidence for the association of *GDF2* mutations with PAH and confirms that these mutations cause impaired BMP9 function

and signaling. Moreover, this study shows for the first time that BMP10 levels are altered in PAH and demonstrates biological integration of plasma BMP9 and BMP10 levels. The findings provide further justification for the use of therapeutic approaches that enhance BMP9 signaling in patients with PAH.

This article has an online data supplement, which is accessible from this issue's table of content online at www.atsjournals.org.

AJRCCM Articles in Press. Published on 29-October-2019 as 10.1164/rccm.201906-1141OC

ABSTRACT

Objectives: Recently, rare heterozygous mutations in *GDF2* were identified in patients with pulmonary arterial hypertension (PAH). *GDF2* encodes the circulating bone morphogenetic protein, BMP9, which is a ligand for the BMP type 2 receptor (BMPR2). Here we determined the functional impact of *GDF2* mutations and characterized plasma BMP9 and BMP10 levels in patients with idiopathic PAH.

Methods: Missense BMP9 mutant proteins were expressed *in vitro* and the impact on BMP9 protein processing and secretion, endothelial signaling and functional activity was assessed. Plasma BMP9 and BMP10 levels and activity were assayed in PAH patients with *GDF2* variants, and controls. Levels were also measured in a larger cohort of controls (n=120) and idiopathic PAH patients (n=260).

Main Results: We identified novel rare variation at the *GDF2* and *BMP10* loci, including copy number variation. *In vitro*, BMP9 missense proteins demonstrated impaired cellular processing and secretion. PAH patients carrying these mutations exhibited reduced plasma levels of BMP9 and reduced BMP activity. Unexpectedly, plasma BMP10 levels were also markedly reduced in these individuals. Although overall BMP9 and BMP10 levels did not differ between PAH patients and controls, BMP10 levels were lower in PAH females. A subset of PAH patients had markedly reduced plasma levels of BMP9 and BMP10 in the absence of *GDF2* mutations.

Conclusions: Our findings demonstrate that *GDF2* mutations result in BMP9 loss-of-function and are likely causal. These mutations lead to reduced circulating levels of both BMP9 and BMP10. These findings support therapeutic strategies to enhance BMP9 or BMP10 signaling in PAH.

INTRODUCTION

Pulmonary arterial hypertension (PAH) is a rare but important life-limiting disease that typically presents with unexplained breathlessness on exertion (1). The lung pathology is characterized by narrowing and obliteration of small pulmonary arteries resulting from proliferation of endothelial cells, smooth muscle cells and fibroblasts in the vessel wall (2). The resulting elevation in pulmonary vascular resistance leads to severe pulmonary arterial hypertension. The pressure-overloaded right ventricle responds initially by hypertrophy, but ultimately dilates and fails (3). Average transplant-free 3-year survival remains only 60-70% despite existing therapies (3, 4), demanding a search for more effective treatments based on a more thorough understanding of the pathobiology.

Human genetic studies have revealed important insights into the pathobiology of PAH. Heterozygous mutations in the gene encoding the bone morphogenetic protein type 2 receptor (*BMPR2*) are the most common genetic cause of PAH, accounting for 53-86% of familial cases and 14-35% of idiopathic cases (5-7). Further cases are accounted for by mutations in activin receptor-like kinase 1 (*ACVRL1* encoding ALK1), Endoglin (*ENG*), and by mutations in genes encoding signaling intermediaries downstream of BMP receptors, such as *SMAD9* (7). Additional rare variants have been described in the genes encoding caveolin-1 (*CAV1*) (8) and the potassium channel, *KCNK3* (9). In a large European cohort study, we provided the first evidence for additional causal mutations in *GDF2* (which encodes BMP9), *ATP13A3* (a P5-type ATPase), *SOX17* (SRY-Box 17) and *AQP1* (aquaporin-1) (10). The identification of *GDF2* mutations has since been independently replicated (11), accounting for 6.7% of idiopathic PAH cases in a Chinese cohort.

It is now known that BMPR2 and ALK1, together with ENG as an accessory receptor, form a BMP signaling complex, largely restricted to endothelial cells (12). Of the 12 different

AJRCCM Articles in Press. Published on 29-October-2019 as 10.1164/rccm.201906-1141OC

BMPs involved in fundamental and diverse cellular functions, only BMP9 and BMP10 are circulating physiological ligands for the BMPR2/ALK1 receptor complex (13). BMP9 is expressed primarily in the liver (14, 15), whereas BMP10 is highly expressed in the right atrium (15, 16). Recent evidence suggests the presence of circulating BMP9/BMP10 heterodimers (15). These BMP ligands circulate at physiologically active levels and maintain vascular endothelial quiescence (17). Moreover, we previously demonstrated that therapeutic administration of BMP9 prevents and reverses PAH in genetic and non-genetic models of disease (12).

Here we sought to determine whether recently identified and novel heterozygous mutations in *GDF2* cause BMP9 loss-of-function, based on biochemical characterization and measurements of BMP9 plasma levels in patients. In addition, we assayed BMP9 and BMP10 levels in a large PAH cohort and demonstrate that a subset of PAH patients, without identified *GDF2* mutations, also exhibit reduced circulating BMP9 and BMP10 levels. Some of these results have been previously reported in the form of abstracts (18, 19).

METHODS

A cohort of 1048 PAH patients underwent whole genome sequencing, and a case-control rare variant analysis was undertaken, as described previously (10). Variants which occurred at a frequency of more than 1 in 10000, or were not predicted to disrupt protein structure according to *in silico* prediction analyses, were classified as likely benign (eTable 3).

We selected 7 missense PAH-associated potentially pathogenic *GDF2* variants and 9 common and/or benign variants for functional comparison. Proteins were expressed as prodomain bound BMP9 (Pro:BMP9) as previously reported (10), generating three batches per variant.

Plasma levels of BMP9 and pBMP10 were measured in 260 patients with idiopathic or heritable PAH, and 120 controls. Patient samples were made available by the UK PAH Cohort (www.ipahcohort.com, https://www.ukctg.nihr.ac.uk, Unique Identifier: NCT01907295). All patients provided written informed consent and the study was approved by the ethics review committee (REC Ref: 13/EE/0203). The control samples were described previously (20).

RESULTS

Identification of *GDF2* mutations

Whole genome sequencing identified 7 likely pathogenic missense variants, and 1 frameshift variant in *GDF2* (n=8) (10). In the present study we searched for additional structural variation at the *GDF2* locus and identified 2 patients with large deletions, not previously described, encompassing the *GDF2* locus and several neighboring genes (Table 1, eFigure 1a). The p.Y351H variant, found in 2 unrelated patients, was not previously reported and is predicted to disrupt the hydrophobic core of BMP9 (eFigure 1b). With the additional 4 carriers identified in this study, we have now identified a total of 12 *GDF2* mutation carriers. Two patients with *GDF2* missense variants (p.M89V and p.Y351H) had a positive family history for PAH, with sufficient information available for the M89V variant carrier to construct a pedigree, although sequencing data were available only for the proband (eFigure 1c).

We compared the demographics and clinical parameters of the *GDF2* mutation carriers (n=12) with patients harboring heterozygous *BMPR2* mutations (n=159) and patients with no identified mutation (n=750) (Table 2). *GDF2* mutation carriers were similar to PAH patients without mutations and showed no features of hereditary hemorrhagic telangiectasia (HHT) or vascular anomaly syndromes. *GDF2* mutation carriers were significantly older and

AJRCCM Articles in Press. Published on 29-October-2019 as 10.1164/rccm.201906-1141OC

had less severe hemodynamics than *BMPR2* mutation carriers. Transplant-free survival was similar between groups after adjustment for age, sex, and whether cases were incident or prevalent. The two patients with large deletions exhibited earlier onset of disease at 19 and 30 years of age (Table 1). The 19-year-old underwent transplantation after 3 years. Despite the deletions affecting several additional genes (eFigure 1), these individuals did not have reported co-morbidities. In addition, we searched for potentially deleterious mutations in BMP10. Two rare and deleterious missense variants in *BMP10* (p.A361E and p.R353C) were identified in PAH patients (eTable 4). The individual carrying p.R353C has been reported previously (21).

Biochemical characterization of BMP9 variants

BMP9 circulates in a non-covalent complex with its prodomain (Figure 1a) (14). We previously reported that missense mutations predicted to be pathogenic *in silico* cluster at the interface of the growth factor and prodomains (10), leading us to hypothesize that they disrupt the Pro:BMP9 complex. We expressed BMP9 variants in vitro which were predicted to be either: (1) deleterious in the PAH cohort, (2) benign in the PAH cohort, (3) deleterious but not exclusive to PAH or, (4) benign and not exclusive to PAH (eTable 3). Measurement of the concentration of BMP9 in conditioned media by ELISA demonstrated that the secretion of pathogenic variants was markedly reduced (Figure 1b). With the exception of P104L (see Discussion), variants predicted to be benign were secreted efficiently. For all detectable variants, the measured absorbances paralleled the standard curve, implying that the ELISA antibodies cross-reacted fully with these variants and reduced detection was not due to epitope change (eFigure 2).

We confirmed the ELISA data by western blotting of conditioned media for the growth factor and prodomains of BMP9 (Figure 1c). For pathogenic variants, there was an

excess of secreted prodomain compared to growth factor domain, indicating that the Pro:BMP9 complex was indeed disrupted (Figure 1d). There was almost no detectable secreted growth factor domain for Pro:BMP9-R110W, -E143K, -Y351H and -T413N despite quantifiable amounts of secreted prodomain. Western blotting of transfected cell lysates revealed that *ProBMP9* was efficiently expressed within cells, but compared to Pro:BMP9-WT, there was a loss of processed species with these pathogenic variants, suggesting reduced stability (Figure 1e).

In addition, we demonstrated a processing defect in the *ProBMP9*-S320C variant, which introduces a substitution immediately adjacent to the furin cleavage site between the growth factor and prodomain (eFigure 3a). The *ProBMP9*-S320C mutation resulted in an excess of uncleaved species accumulating in conditioned media (eFigure 3b). Within cell lysates, equal amounts of both unprocessed *ProBMP9*-WT and -S320C were present (eFigure 3b), indicating a defect during secretion.

We confirmed that the BMP9 prodomain is glycosylated (eFigure3c-e) and the increased molecular weight of the prodomain of the common D218N variant is due to an additional *de novo* glycosylation site, which does not alter function (Figure 2).

Assessment of signaling and functional capacity of BMP9 variants

We undertook a functional assessment of the signaling activity of BMP9 variants in conditioned media using hALK1-transfected C2C12 cells, which exhibit a concentration-response to 10-100 pg/ml of BMP9 (eFigure 4). All secreted growth factor domains had potency equivalent to Pro:BMP9-WT (Figure 2a). There was no activity associated with conditioned media containing pathogenic variants with negligible detectable growth factor domain (Figure 2b, eFigure 5). Similarly, for Pro:BMP9-M89V, activity assays suggested a reduced amount of growth factor domain compared to prodomain. The transcriptional activity

AJRCCM Articles in Press. Published on 29-October-2019 as 10.1164/rccm.201906-1141OC

of BMP9 variants in BOECs (22) was consistent with the ALK1-luciferase experiments (Figure 2c,d).

Finally, we assessed the anti-apoptotic activity of benign and pathogenic variants on BOECs by flow-cytometry (Figure 2e)(12). Due to the limited through-put of this approach, we screened all the mutants for their capacity to inhibit apoptosis of human pulmonary artery endothelial cells (PAECs) by Caspase-GLO® 3/7 assays (Figure 2f,g). These also showed most variants possessed anti-apoptotic activity, except for the pathogenic variants which lead to a profound loss of secreted growth factor domain, despite the presence of prodomain, which had no anti-apoptotic activity.

PAH patients carrying pathogenic *GDF2* alleles exhibit reduced circulating BMP9 and BMP10 levels and plasma BMP activity

Using a BMP9 ELISA protocol validated for lack of cross-reactivity (eFigure 6a), spike recovery (eFigure 6b-g) and plasma assay diluents (eFigure 6b-h), we measured circulating BMP9 plasma levels and activity in patients carrying *GDF2* mutations. Plasma from female PAH patients who were heterozygous carriers of either benign (Pro:BMP9-G18V, -G74E, -R82G, -P104L, -I118F, -V154I, -D218N, -G291S, -E297K, -T304M, -R333W) or pathogenic (Pro:BMP9-M89V, -A347V, -Y351H, -T413N) alleles, were compared to samples from age-matched healthy females. Patients carrying pathogenic missense *GDF2* variants had significantly lower mean plasma BMP9 levels than controls, whereas no significant reduction was evident in PAH patients carrying benign variants (Figure 3a). Similarly, PAH patients carrying deletions at the *GDF2* locus, or the frameshift mutation, exhibited reduced levels of plasma BMP9.

To determine whether reduced BMP9 levels led to reduced plasma activity, we exposed HMEC1-BRE luciferase cells, which demonstrate high affinity responses to BMP9

(eFigure 7), to plasma (Figure 3b). The BMP activity of plasma followed a similar pattern to measured BMP9 concentrations, such that patients with pathogenic missense mutations or deletions exhibited reduced activity. Following BMP9 immunoprecipitation in control plasma there was reduced activity, confirming that BMP9 is responsible for the majority of plasma BMP activity in this assay.

In addition, we used a pBMP10 ELISA protocol validated for lack of cross-reactivity (eFigure 8a), spike recovery and plasma diluents (eFigure 8b-d), to measure circulating pBMP10 plasma levels in patients carrying *GDF2* mutations. Remarkably, plasma BMP10 levels were dramatically reduced in BMP9 mutation carriers (Figure 3c). Moreover, plasma BMP9 and pBMP10 levels correlated closely, both in controls and in mutation carriers (Figure 3d).

Plasma BMP9 and pBMP10 levels in IPAH and HPAH patients

We next measured BMP9 and pBMP10 levels in 120 control samples and 260 cases of heritable or idiopathic PAH (eTable 5). Levels of BMP9 and pBMP10 were significantly higher in females than males in both control and PAH groups (Figure 4a). Levels of ligands were not associated with age (eFigure 9). No significant differences were observed in the plasma levels of BMP9 between PAH patients and controls of the same sex (Figure 4a). Although no difference in pBMP10 levels was observed between male controls and male PAH patients, pBMP10 levels in females with PAH were significantly lower than control females (Figure 4b). When the BMP9 or pBMP10 levels in PAH patients and controls of each sex were pooled, PAH patients were overrepresented by two-fold in the lowest quartile of either BMP9 or pBMP10 levels, in both males and females (eTable 6). Moreover, a larger proportion of male (14/21 for BMP9 and 14/20 for pBMP10) and female (38/56) PAH patients shared both BMP9 and pBMP10 levels in their lowest quartiles compared to control

AJRCCM Articles in Press. Published on 29-October-2019 as 10.1164/rccm.201906-1141OC

males (1/7) and control females (8/77*)*. We confirmed the reduction of BMP9 in these samples by ELISA and confirmed reduced activity for inducing *ID1* and *ID2* transcription in endothelial cells (Figure 4c). Consistent with our observation in *GDF2* mutation carriers, there was a striking correlation between plasma BMP9 and pBMP10 in control subjects ((Figure 4d), Spearman r = 0.72, 95% CI [0.61;0.80] *P*<0.0001) and in PAH patients ((Figure 4e), Spearman r = 0.75, 95% CI [0.68;0.80], *P*<0.0001).

We hypothesized that a physical association between BMP9 and pBMP10 could explain the correlation in measured levels. Immunoprecipitation of BMP9 and BMP10 from control samples, followed by ELISA and activity measurements demonstrated that a proportion of circulating BMP9 and pBMP10 are physically associated (eFigure 10). Since most circulating activity was associated with BMP9, but measured levels of pBMP10 were much higher than levels of BMP9, we hypothesized that endogenous pBMP10 is predominately unprocessed *ProBMP10.* Therefore, we compared the immunoreactivity of purified *ProBMP10* and Pro:BMP10 in the pBMP10 and BMP10 GFD ELISAs (eFigure 11a,b). This demonstrated that the pBMP10 ELISA detects unprocessed and processed pBMP10, whilst the BMP10 GFD ELISA only detects processed Pro:BMP10. In control samples, very little endogenous processed Pro:BMP10 was detectable with the BMP10 GFD ELISA, despite efficient spike-recovery, which suggests that endogenous pBMP10 is indeed unprocessed (eFigure 11c).

Associations between BMP9 and 10 levels and clinical parameters

We compared clinical characteristics between BMP9 (eTable7) and pBMP10 (eTable8) tertiles and also undertook correlation analysis for relationships (continuous variables) between ligand concentrations and clinical parameters. In PAH patients, BMP9 and pBMP10 levels were not associated with exercise capacity measured by 6-minute walk test (6MWT)

(r=-0.045, 95% CI [-0.22;0.13], p=0.634 and r=0.15, 95% CI [-0.032;0.32], p=0.106 respectively). Hemodynamics contemporary to the time of sampling were available for 38 patients but did not show any correlation with BMPs. Of note, BMP9 and pBMP10 levels negatively correlated with BMI in PAH cases but not in controls (eFigure 12).

Analysis of clinical blood tests in the PAH cohort revealed that pBMP10 negatively correlated with red cell distribution width (RDW) (r= -0.21, 95% CI [-0.35;-0.06], p=0.006) and alkaline phosphatase activity (r= -0.16, 95% CI [-0.28;-0.03], p=0.014) and positively with albumin concentration (r= 0.32, 95% CI [0.20;0.43], p<0.001), whereas BMP9 levels correlated positively with platelet count (r= 0.18, 95% CI [0.05;0.30], p=0.006). Both BMP9 and pBMP10 correlated negatively with CRP (r= -0.32, 95% CI [-0.45;-0.18], p<0.001; r=-0.35, 95% CI [-0.47;-0.20], p<0.001 respectively). Binary logistic regression showed that plasma pBMP10 concentrations were significantly negatively associated with systemic hypertension even after controlling for BMI and sex in the PAH cohort. When pBMP10 levels were in the lower tertile the log odds ratio of suffering from systemic hypertension were, -1.30 95% CI [-2.21;-0.49]. Low pBMP10 concentrations were also predictive of diabetes mellitus type 2, but this association disappeared after controlling for BMI and sex. Receiver operating characteristics (ROC) curves (eFigure 13) suggested that the cut-off values of 6784.7pg/ml (specificity 46.3%, sensitivity 79.2%, AUC 63.8%) and 6180.1pg/ml (specificity 51.9%, sensitivity 78.9%, AUC 66%) (data for PAH) were the most discriminative to predict systemic hypertension and diabetes mellitus respectively. However, the AUC was low for both diseases, indicating a modest predictive capacity. Circulating BMP9 levels were not associated with either diabetes mellitus or systemic hypertension.

During the median follow up of 4.4 years since sampling 48 (19%) PAH patients died, resulting in a 1 and 3 years overall survival of 95% and 86%. Neither BMP9 nor pBMP10 concentrations were predictive of mortality (eFigure 14).

AJRCCM Articles in Press. Published on 29-October-2019 as 10.1164/rccm.201906-1141OC

DISCUSSION

In this study we provide a detailed functional analysis of rare potentially damaging mutations in *GDF2* identified in a large European cohort of PAH patients. The majority of mutations lead to altered cellular processing of the mature protein and reduced cellular secretion. The mutations were associated with reduced circulating levels of BMP9 in these individuals and reduced plasma BMP9 activity. These findings support a causal role for these mutations in the pathobiology of PAH and provide strong evidence in humans that reduced BMP9 levels and activity promote the development of PAH. In addition, the finding of two patients with deletions at the *GDF2* locus provides new genetic evidence supporting a causal role in PAH.

Having identified several likely causal missense *GDF2* variants based on *in silico* analyses, we went on to functionally characterize these variants. Our observations confirm that the Pro:BMP9-M89V, -R110W, -E143K, -S320C, -A347V, -Y351H and -T413N mutations exhibit impaired BMP9 processing, secretion or stability. Those mutants predicted to be benign functioned normally *in vitro*, but the common Pro:BMP9-D218N variant, predicted to be deleterious *in silico*, was functionally normal. One exception was Pro:BMP9-P104L, which was predicted to be deleterious, but functional analysis suggested it is likely to be benign. This variant was secreted less efficiently from transfected cells but was not disrupted to the same extent as the pathogenic mutants, such that it exhibited normal processing and signaling, and the individual carrying this variant had normal plasma levels of BMP9. The clustering of pathogenic mutations around the interface between the BMP9 growth factor and prodomains suggests that destabilization of the BMP9 protein, exemplified by the Pro:BMP9-M89V variant, is an important mechanism. The S320C variant, which is altered at the prohormone cleavage site, exhibits a processing cleavage defect, confirming a recent study of the same mutation (11). These results highlight the importance of careful characterization of missense variants before pathogenicity can be confirmed.

Two recent studies independently validated the original finding of heterozygous *GDF2* mutations in PAH cohorts (11, 21). A single previous case report had identified a case of childhood-onset PAH harboring a homozygous *GDF2* truncating mutation (p.Q26X) (23). In a Chinese PAH cohort the authors measured plasma BMP9 by ELISA in 19 *GDF2* mutation carriers compared with age- and sex-matched idiopathic PAH patients and healthy controls (11). Median plasma BMP9 levels were significantly reduced in idiopathic PAH patients and were lowest in patients carrying *GDF2* mutations. In our larger analysis of a cohort of controls and IPAH patients, we did not observe a significant difference in overall BMP9 levels between controls and idiopathic PAH patients. However, we observed that some patients with idiopathic PAH (approx. 5.4%) have very low BMP9 levels, unexplained by the presence of mutations, with corresponding reduced plasma BMP activity on endothelial cells. A recent study found that patients with portopulmonary hypertension have profound reductions in plasma BMP9 and that low levels predict the presence of PAH in cirrhosis patients (24). Liver disease was specifically excluded in the idiopathic PAH patients recruited to our cohort. Taken together, the genetic and non-genetic evidence in humans suggests that loss of BMP9 levels, or BMP9 signaling, is an important driver for the development of PAH. The observed difference between plasma levels of BMP9 (and pBMP10) in males and females is of interest and the underlying mechanism for this difference warrants further study. Although higher levels in females superficially conflicts with the observation that idiopathic and heritable PAH more commonly affects females, the prognosis of PAH is usually worse in male patients.

To our knowledge, ours is the first study to measure plasma levels of BMP10 in PAH patients, or indeed in a large cohort of control subjects. Overall, levels of pBMP10 were significantly lower in female PAH patients compared with controls. Remarkably, we observed a close correlation between the levels of BMP9 and BMP10 in human plasma,

AJRCCM Articles in Press. Published on 29-October-2019 as 10.1164/rccm.201906-1141OC

suggesting a degree of co-regulation that might be explained, at least in part, by the presence of circulating heterodimers of these ligands (15). This is important because *GDF2* mutations leading to reduced secretion of ligand would be predicted to impact the circulating levels of BMP10, as well as BMP9, as observed in this study. We confirmed by immunoprecipitation that a proportion BMP9 and pBMP10 are physically associated in the same complex. However, we measured levels of pBMP10 by ELISA that were much higher than BMP9, which suggests the association is not 1:1. Additionally, only about half of the plasma BMP9 and pBMP10 were in complex, implying that BMP9:10 heterodimers cannot represent the only active form. Intriguingly, we detected appreciable levels of circulating processed Pro:BMP9 by ELISA, associated with high activity on cells, but minimal circulating processed Pro:BMP10. This suggests that the majority of circulating pBMP10 is unprocessed. The potentially important role of BMP10 in PAH is further supported by the finding of two individuals with likely pathogenic missense mutations, providing independent validation of the previous report of *BMP10* mutations from France (21). Unfortunately, plasma was not available from these individuals for further analysis.

The human data presented here are important because a recent study in rodents suggested that inhibition of BMP9 signaling might be protective against the development of pulmonary hypertension (25). *Gdf2* knockout mice do not develop spontaneous pulmonary hypertension, but the authors found that *Gdf2* knockout mice were protected from the development of hypoxia-induced pulmonary hypertension. They went on to show that inhibition of Bmp9 signaling with a neutralizing anti-BMP9 antibody could also slightly prevent the development of pulmonary hypertension during chronic hypoxia. Their results directly conflict with another study showing that inhibition of BMP9 and 10 with Fc-ALK1 exacerbated pulmonary hypertension during chronic hypoxia (24). Taken together, the human genetic evidence (10, 11, 21, 23), and data from patients with cirrhosis (24), supports the

view that BMP9 and 10 are protective to the pulmonary vascular endothelium, consistent with the beneficial effects of therapeutic supplementation of BMP9 in preclinical models (12).

Heterozygous *GDF2* mutations have been identified previously in a small number of patients with a vascular anomaly syndrome resembling hereditary hemorrhagic telangiectasia (HHT) (26, 27). The mutations in HHT patients were distinct from those reported in PAH but were also predicted to lead to altered cellular processing. The finding of mutations in *GDF2* in both HHT-like syndromes and PAH is perhaps not surprising given that mutations in the endothelial receptor for BMP9, ALK1, can also cause either HHT or PAH (28). Of note, none of the patients carrying *GDF2* mutations in the present study had clinical features of HHT.

In summary, the present study demonstrates that rare heterozygous mutations in *GDF2* are loss-of-function and likely causal in the pathobiology of PAH. Furthermore, *GDF2* mutations lead to reduced circulating levels of BMP10, as well as BMP9, supporting a degree of co-regulation of these ligands. Taken together, these findings further support the central role of the BMP9/BMPR2/ALK1 axis in PAH.

AJRCCM Articles in Press. Published on 29-October-2019 as 10.1164/rccm.201906-1141OC

Acknowledgements

The UK National Institute for Health Research BioResource—Rare Diseases (NIHR BR-RD) and the BHF/MRC UK National Cohort of Idiopathic and Heritable PAH made this study possible. We gratefully acknowledge the participation of patients recruited to the NIHR BR-RD. We thank the NIHR BR-RD staff and co-ordination teams at the University of Cambridge, and the research nurses and coordinators at the specialist pulmonary hypertension centres involved in this study. We acknowledge the support of the Imperial NIHR Clinical Research Facility, the Netherlands CardioVascular Research Initiative, the Dutch Heart Foundation, Dutch Federation of University Medical Centres, the Netherlands Organisation for Health Research and Development and the Royal Netherlands Academy of Sciences. We thank all the patients and their families who contributed to this research and the Pulmonary Hypertension Association (UK) for their support. The UK National Cohort of Idiopathic and Heritable PAH is supported by the NIHR, the British Heart Foundation (BHF) (SP/12/12/29836), the BHF Cambridge Centre of Cardiovascular Research Excellence, the UK Medical Research Council (MR/K020919/1), the Dinosaur Trust, NIHR Great Ormond Street Hospital Biomedical Research Centre, Great Ormond Street Hospital Charity, BHF Programme grants to RCT (RG/08/006/25302) and NWM (RG/13/4/30107), and the UK NIHR Cambridge Biomedical Research Centre. JH is funded through a BHF 4-year PhD programme (FS/15/62/323032). NWM is a BHF Professor and NIHR Senior Investigator. CH is a NIHR Rare Disease Translational Research Collaboration Clinical PhD Fellow. LS is supported by the Wellcome Trust Institutional Strategic Support Fund (204809/Z/16/Z) awarded to St. George's, University of London. CJR is supported by a BHF Intermediate Basic Science Research Fellowship (FS/15/59/31839). AL is supported by a BHF Senior Basic Science Research Fellowship (FS/13/48/30453 and FS/18/52/33808). This work was supported in part by the Assistance Publique-Hôpitaux de Paris, Inserm, Université Paris-

Sud, and Agence Nationale de la Recherche (Département Hospitalo-Universitaire Thorax Innovation; LabEx LERMIT, ANR-10-LABX-0033; and RHU BIO-ART LUNG 2020, ANR-15-RHUS-0002).

AJRCCM Articles in Press. Published on 29-October-2019 as 10.1164/rccm.201906-1141OC

REFERENCES

1. Farber HW, Loscalzo J. Pulmonary arterial hypertension. *N Engl J Med* 2004;351:1655-1665.

2. Tuder RM, Archer SL, Dorfmüller P, Erzurum SC, Guignabert C, Michelakis E, Rabinovitch M, Schermuly R, Stenmark KR, Morrell NW. Relevant issues in the pathology and pathobiology of pulmonary hypertension. *J Am Coll Cardiol* 2013;62:D4-12.

3. Thenappan T, Ormiston ML, Ryan JJ, Archer SL. Pulmonary arterial hypertension: Pathogenesis and clinical management. *Bmj-Brit Med J* 2018;360.

4. Evans JDW, Girerd B, Montani D, Wang X-J, Galiè N, Austin ED, Elliott G, Asano K, Grünig E, Yan Y, Jing Z-C, Manes A, Palazzini M, Wheeler LA, Nakayama I, Satoh T, Eichstaedt C, Hinderhofer K, Wolf M, Rosenzweig EB, Chung WK, Soubrier F, Simonneau G, Sitbon O, Gräf S, Kaptoge S, Di Angelantonio E, Humbert M, Morrell NW. *BMPR2* mutations and survival in pulmonary arterial hypertension: An individual participant data meta-analysis. *Lancet RespirMed* 2016;4:129-137.

5. Morrell NW, Aldred MA, Chung WK, Elliott CG, Nichols WC, Soubrier F, Trembath RC, Loyd JE. Genetics and genomics of pulmonary arterial hypertension. *Eur Respir J* 2019;53:1801899.

6. Soubrier F, Chung WK, Machado R, Grünig E, Aldred M, Geraci M, Loyd JE, Elliott CG, Trembath RC, Newman JH, Humbert M. Genetics and genomics of pulmonary arterial hypertension. *J Am Coll Cardiol* 2013;62:D13-21.

7. Machado RD, Southgate L, Eichstaedt CA, Aldred MA, Austin ED, Best DH, Chung WK, Benjamin N, Elliott CG, Eyries M, Fischer C, Gräf S, Hinderhofer K, Humbert M, Keiles SB, Loyd JE, Morrell NW, Newman JH, Soubrier F, Trembath RC, Viales RR, Grünig E. Pulmonary arterial hypertension: A current perspective on established and emerging molecular genetic defects. *HumMutat* 2015;36:1113-1127.

8. Austin ED, Ma L, LeDuc C, Berman Rosenzweig E, Borczuk A, Phillips JA, 3rd, Palomero T, Sumazin P, Kim HR, Talati MH, West J, Loyd JE, Chung WK. Whole exome sequencing to identify a novel gene (caveolin-1) associated with human pulmonary arterial hypertension. *CircCardiovascGenet* 2012;5:336-343.

9. Ma L, Roman-Campos D, Austin ED, Eyries M, Sampson KS, Soubrier F, Germain M, Trégouët D-A, Borczuk A, Rosenzweig EB, Girerd B, Montani D, Humbert M, Loyd JE, Kass RS, Chung WK. A novel channelopathy in pulmonary arterial hypertension. *N Engl J Med* 2013;369:351-361.

10. Gräf S, Haimel M, Bleda M, Hadinnapola C, Southgate L, Li W, Hodgson J, Liu B, Salmon RM, Southwood M, Machado RD, Martin JM, Treacy CM, Yates K, Daugherty LC, Shamardina O, Whitehorn D, Holden S, Aldred M, Bogaard HJ, Church C, Coghlan G, Condliffe R, Corris PA, Danesino C, Eyries M, Gall H, Ghio S, Ghofrani H-A, Gibbs JSR, Girerd B, Houweling AC, Howard L, Humbert M, Kiely DG, Kovacs G, MacKenzie Ross RV, Moledina S, Montani D, Newnham M, Olschewski A, Olschewski H, Peacock AJ, Pepke-Zaba J, Prokopenko I, Rhodes CJ, Scelsi L, Seeger W, Soubrier F, Stein DF, Suntharalingam J, Swietlik EM, Toshner MR, van Heel DA, Vonk Noordegraaf A, Waisfisz Q, Wharton J, Wort SJ, Ouwehand WH, Soranzo N, Lawrie A, Upton PD, Wilkins MR, Trembath RC, Morrell NW. Identification of rare sequence variation underlying heritable pulmonary arterial hypertension. *Nat Commun* 2018;9:1416.

11. Wang XY, Lian TY, Jiang X, Liu SF, Li SQ, Jiang R, Wu WH, Ye J, Cheng CY, Du Y, Xu XQ, Wu Y, Peng FH, Sun K, Mao YM, Yu H, Liang C, Shyy JY, Zhang SY, Zhang X, Jing JC. Germline BMP9 mutation causes idiopathic pulmonary arterial hypertension. *Eur Respir J* 2019;53:1-10.

12. Long L, Ormiston ML, Yang X, Southwood M, Gräf S, Machado RD, Mueller M, Kinzel B, Yung LM, Wilkinson JM, Moore SD, Drake KM, Aldred MA, Yu PB, Upton PD, Morrell NW. Selective enhancement of endothelial BMPR-II with BMP9 reverses pulmonary arterial hypertension. *NatMed* 2015;21:777-785.

AJRCCM Articles in Press. Published on 29-October-2019 as 10.1164/rccm.201906-1141OC

13. David L, Mallet C, Mazerbourg S, Feige JJ, Bailly S. Identification of bmp9 and bmp10 as functional activators of the orphan activin receptor-like kinase 1 (ALK1) in endothelial cells. *Blood* 2007;109:1953-1961.

14. Bidart M, Ricard N, Levet S, Samson M, Mallet C, David L, Subileau M, Tillet E, Feige JJ, Bailly S. BMP9 is produced by hepatocytes and circulates mainly in an active mature form complexed to its prodomain. *Cell MolLife Sci* 2012;69:313-324.

15. Tillet E, Ouarné M, Desroches-Castan A, Mallet C, Subileau M, Didier R, Lioutsko A, Belthier G, Feige J-J, Bailly S. A heterodimer formed by bone morphogenetic protein 9 (BMP9) and BMP10 provides most bmp biological activity in plasma. *J Biol Chem* 2018;293:10963-10974.

16. Jiang H, Salmon RM, Upton PD, Wei Z, Lawera A, Davenport AP, Morrell NW, Li W. The prodomain-bound form of bone morphogenetic protein 10 is biologically active on endothelial cells. *J Biol Chem* 2016;291:2954-2966.

17. David L, Mallet C, Keramidas M, Lamande N, Gasc JM, Dupuis-Girod S, Plauchu H, Feige JJ, Bailly S. Bone morphogenetic protein-9 is a circulating vascular quiescence factor. *CircRes* 2008;102:914-922.

18. Swietlik E, Hodgson J, Hadinnapola C, Bleda M, Haimel M, Church C, Coghlan G, Condliffe R, Corris P, Gibbs J, Holden S, Howard L, Humbert M, Jonson M, Kiely D, Lawrie A, Lordan J, MacKenzie Ross R, Olschewski H, Moledina S, Peacock A, Pepke-Zaba J, Suntharalingam J, Seeger W, Toshner M, Trembath R, Vonk Noordegraaf A, Wharton J, Wilkins M, Wort S, Upton P, Gräf S, Morrell N. S40 phenotypic characterisation of *GDF2* mutation carriers in a large cohort of patients with pulmonary arterial hypertension. *Thorax* 2018;73:A24-A26.

19. Hodgson J, Swietlik E, Salmon R, Hadinnapola C, Wharton J, Haimel M, Bleda M, Lawera A, Li W, Wilkins M, Gräf S, Upton P, Morrell N. S41 characterisation of mutations in the gene encoding growth and differentiation factor 2 (*GDF2*) in patients with pulmonary arterial hypertension. *Thorax* 2018;73:A26-A26.

20. Rhodes CJ, Ghataorhe P, Wharton J, Rue-Albrecht KC, Hadinnapola C, Watson G, Bleda M, Haimel M, Coghlan G, Corris PA, Howard LS, Kiely DG, Peacock AJ, Pepke-Zaba J, Toshner MR, Wort SJ, Gibbs JSR, Lawrie A, Gräf S, Morrell NW, Wilkins MR. Plasma metabolomics implicates modified transfer RNAs and altered bioenergetics in the outcomes of pulmonary arterial hypertension. *Circulation* 2017;135:460-475.

21. Eyries M, Montani D, Nadaud S, Girerd B, Levy M, Bourdin A, Tresorier R, Chaouat A, Cottin V, Sanfiorenzo C, Prevot G, Reynaud-Gaubert M, Dromer C, Houeijeh A, Nguyen K, Coulet F, Bonnet D, Humbert M, Soubrier F. Widening the landscape of heritable pulmonary hypertension mutations in paediatric and adult cases. *Eur Respir J* 2019;53:1801371.

22. Toshner M, Dunmore BJ, McKinney EF, Southwood M, Caruso P, Upton PD, Waters JP, Ormiston ML, Skepper JN, Nash G, Rana AA, Morrell NW. Transcript analysis reveals a specific HOX signature associated with positional identity of human endothelial cells. *PloS one* 2014;9:e91334.

23. Wang G, Fan R, Ji R, Zou W, Penny DJ, Varghese NP, Fan Y. Novel homozygous BMP9 nonsense mutation causes pulmonary arterial hypertension: A case report. *BMC Pulm Med* 2016;16:17.

24. Nikolic I, Yung L-M, Yang P, Malhotra R, Paskin-Flerlage SD, Dinter T, Bocobo GA, Tumelty KE, Faugno AJ, Troncone L, McNeil ME, Huang X, Coser KR, Lai CSC, Upton PD, Goumans MJ, Zamanian RT, Elliott CG, Lee A, Zheng W, Berasi SP, Huard C, Morrell NW, Chung RT, Channick RW, Roberts KE, Yu PB. Bone morphogenetic protein 9 is a mechanistic biomarker of portopulmonary hypertension. *Am J Respir Crit Care Med* 2019;199:891-902.

25. Tu L, Desroches-Castan A, Mallet C, Guyon L, Cumont A, Phan C, Robert F, Thuillet R, Bordenave J, Sekine A, Huertas A, Ritvos O, Savale L, Feige J-J, Humbert M, Bailly S, Guignabert C. Selective BMP-9 inhibition partially protects against experimental pulmonary hypertension. *CircRes* 2019.

AJRCCM Articles in Press. Published on 29-October-2019 as 10.1164/rccm.201906-1141OC

26. Wooderchak-Donahue WL, McDonald J, O'Fallon B, Upton PD, Li W, Roman BL, Young S, Plant P, Fülöp GT, Langa C, Morrell NW, Botella LM, Bernabeu C, Stevenson DA, Runo JR, Bayrak-Toydemir P. BMP9 mutations cause a vascular-anomaly syndrome with phenotypic overlap with hereditary hemorrhagic telangiectasia. *Am J Hum Genet* 2013;93:530-537.

27. Hernandez F, Huether R, Carter L, Johnston T, Thompson J, Gossage JR, Chao E, Elliott AM. Mutations in *RASA1* and *GDF2* identified in patients with clinical features of hereditary hemorrhagic telangiectasia. *HumGenome Var* 2015;2:15040.

28. Trembath RC, Thomson JR, Machado RD, Morgan NV, Atkinson C, Winship I, Simonneau G, Galie N, Loyd JE, Humbert M, Nichols WC, Morrell NW, Berg J, Manes A, McGaughran J, Pauciulo M, Wheeler L. Clinical and molecular genetic features of pulmonary hypertension in patients with hereditary hemorrhagic telangiectasia. *NEnglJMed* 2001;345:325-334.

ID	**E013254**	**E005056**	**E006312**	**E010660**	**E000837**	**E010643**	**E012223**	**E001147**	**E004186**	**W000134**	**E011142**	**W000048**
Nucleotide change	*c.137_150 delGTGGGC TGCCTGAG*	*c.265A>G*	*c.328C>T*	*c.347A>T*	*c.427G>A*	*c.958A>T*	*c.1040C>T*	*c.1051T>C*	*c.1051T>C*	*c.1238C>A*	*del Chr10: 47536678 – 51819820*	*del Chr10: 47535814 – 51823146*
Protein change	p.Gly46Ala fsTer21	p.Met89Val (M89V)	p.Arg110Trp (R110W)	p.Asp116Val (D116V)	p.Glu143Lys (E143K)	p.Ser320Cys (S320C)	p.Ala347Val (A347V)	p.Tyr351His (Y351H)	p.Tyr351His (Y351H)	p.Thr413Asn (T413N)	N/A	N/A
Consequence	Frameshift variant	Missense variant	Missense variant	Missense variant	Missense variant	Missense variant	Missense variant	Missense variant	Missense variant	Missense variant	Large deletion (4.28Mbp)	Large deletion (4.29Mbp)
Ethnicity	European	European	European	European	European	South-Asian	European	European	European	Other	European	South-Asian
Age at diagnosis	45	53	46	52	45	56	30	73	45	54	19	30
Sex	male	female	female	male	male	male	female	female	female	female	male	female
WHO FC	3	3	2	3	n.d	3	3	3	2	3	4	2
Exercise capacity	470 (6WMT)	432 (6MWT)	588 (6MWT)	395 (6MWT)	n.d	403 (6MWT)	220 (Shuttle)	160 (6MWT)	420 (6MWT)	374 (6MWT)	280 (Shuttle)	405 (6MWT)
mPAP [mmHg]	46	34	38	55	52	56	53	59	73	50	n.d.	55
PAWP [mmHg]	16	8	5	9	10	7	n.d	13	9	7	n.d.	8
PVR [WU]	5.8	8.7	6.9	15	8.4	9.4	n.d	11	15	15	n.d.	4.66
CO [L/min]	5	3	4.8	3	5	5.2	4.87	4.1	4.2	2.8	n.d.	10

AJRCCM Articles in Press. Published on 29-October-2019 as 10.1164/rccm.201906-1141OC

Family history	No	Yes	No	No	No	No	No	Yes*	No	No	No	No

Table 1: Gene Changes, Demographics and Pulmonary Hemodynamic Data for PAH Patients Harboring BMP9 Mutations. *Abbreviations:* WHO FC – World Health Organization Functional Class, mPAP – mean pulmonary artery pressure, PVR – pulmonary vascular resistance, CO – cardiac output. n.d.- not done. *A relative in the parental generation was affected, but there is not enough information to draw a pedigree.

	BMPR2 **N=159**	***GDF2*** **N=12**	**No known PAH-causal mutation N=750**	**p-value**	**N**
Sex: ‡				0.357	921
female	105 (66%)	7 (58%)	530 (71%)		
Age [years] †	39 [32;51]	46 [41;54]	52 [39;66]	<0.001	921
Diagnosis: ‡				<0.001	921
HPAH	51 (32.1%)	2 (16.7%)	7 (0.93%)		
IPAH	108 (67.9%)	10 (83.3%)	743 (99.1%)		
WHO class: ‡				.	895
1	2 (1%)	0 (0%)	15 (2%)		
2	31 (20%)	3 (27%)	140 (19%)		
3	95 (60%)	7 (64%)	482 (66%)		
4	30 (19%)	1 (9%)	89 (12%)		
Ethnicity: ‡				0.328	921
African	2 (1.26%)	0 (0.00%)	20 (2.67%)		
East-Asian	1 (0.63%)	0 (0.00%)	7 (0.93%)		
European	136 (85.5%)	9 (75.0%)	638 (85.1%)		
Finnish-European	0 (0.00%)	0 (0.00%)	1 (0.13%)		
Other	14 (8.81%)	1 (8.33%)	38 (5.07%)		

AJRCCM Articles in Press. Published on 29-October-2019 as 10.1164/rccm.201906-1141OC

South-Asian	6 (3.77%)	2 (16.7%)	46 (6.13%)		
mPAP [mmHg] †	58 [52;68]	53 [48;56]	52 [43;61]	<0.001	877
mPAWP [mmHg] †	9 [7;12]	8 [7;10]	9 [7;12]	0.931	780
PVR[WU] †	14 [11;20]	10 [9;15]	10 [7;14]	<0.001	754
CO[L/min] †	3.3 [2.7;4.0]	4.7 [3.5;4.9]	4.0 [3.3;5.1]	<0.001	842
NO challenge: ‡				<0.001	373
non-responder	78 (100%)	4 (100%)	245 (84%)		
vasoresponder	0 (0%)	0 (0%)	46 (16%)		
KCO [% pred.] †	82 [74;94]	68 [67;71]	69 [49;84]	<0.001	546
Hb [g/l] †	162 [151;173]	140 [132;153]	150 [136;163]	<0.001	702
Hct [l/l] †	0.5 [0.5;0.5]	0.4 [0.4;0.4]	0.5 [0.4;0.5]	<0.001	575
WBC [x10e9/l] †	9 [7;10]	7 [7;8]	8 [7;10]	0.013	696
Plt [x10e9/l] †	211 [170;251]	225 [208;256]	228 [185;276]	0.079	693
ALP [IU/l] †	75 [62;104]	78 [70;90]	87 [69;113]	0.010	675
Bilirubin [µmol/l] †	18 [12;26]	8 [8;13]	14 [10;22]	0.001	671

WHO FC – World Health Organization Functional Class, mPAP – mean pulmonary artery pressure, mPAWP – mean pulmonary artery wedge pressure, PVR – pulmonary vascular resistance, NO challenge – Nitric Oxide challenge, KCO – transfer coefficient, Hb- hemoglobin, Hct – hematocrit, WBC – white blood cells, Plt – platelets, ALP – alkaline phosphatase.

Table 2: Clinical characteristics of *BMPR2* and *GDF2* mutation carriers and patients without these mutations. None of the patients showed features of hereditary hemorrhagic

telangiectasia. Data are presented as either † median [interquartile range] or ‡ count (%). p-values represent the overall comparison across the three patient groups.

AJRCCM Articles in Press. Published on 29-October-2019 as 10.1164/rccm.201906-1141OC

Figure 1

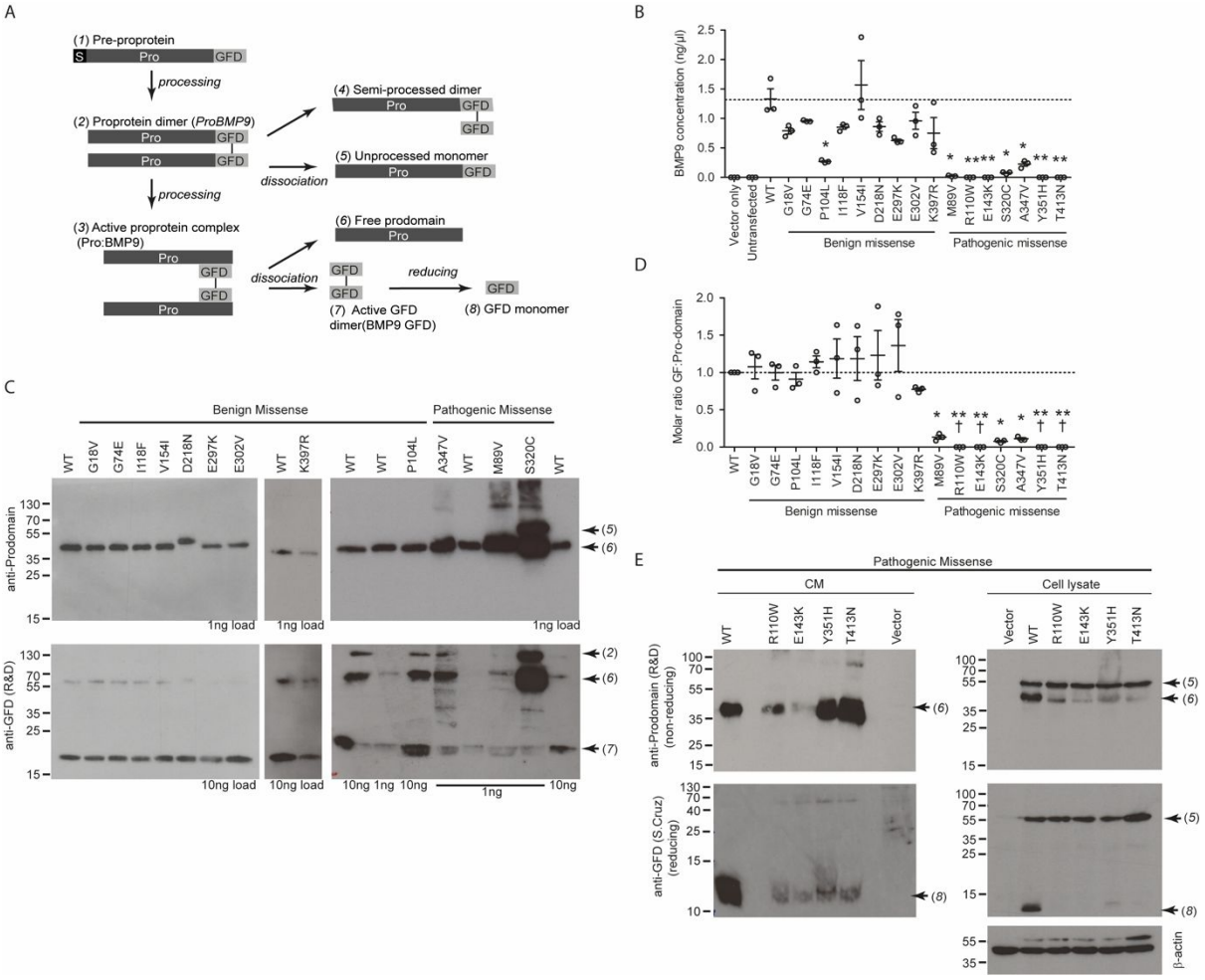

Figure 1: Characterisation of Expressed BMP9 Mutant Proteins. (a) Schematic of different potential species of BMP9. Numbers in brackets correspond to labels on western blots. (b) Conditioned media from HEK-EBNA cells expressing Pro:BMP9-WT or missense pBMP9 variants were serially diluted and assayed for BMP9 GFD levels by ELISA. Data are the mean ± SEM from three independently generated batches of media. Paired Dunnett's multiple comparisons test; **P*<0.05, ***P*<0.01 (c) Western blots of variants in conditioned media in non-reducing conditions. The volume loaded was normalized according to concentration based on ELISA. Blots are representative of n=3 separate expression batches.

(d) The ratio of the band intensities of the growth factor and prodomain for each mutant was normalized to WT. † indicates mutants for which GFD concentration was too low to quantify. Data are the mean ± SEM from three independently generated batches of media. Paired Dunnett's multiple comparisons test; **P*<0.05, ***P*<0.01 (e) Western blotting of those variants not readily detected by ELISA. Cell lysates (30 μg of total protein) and conditioned media (3 μl of Pro:BMP9-WT or 45 μl of Pro:BMP9 mutants and media from the empty vector control) were loaded**.**

AJRCCM Articles in Press. Published on 29-October-2019 as 10.1164/rccm.201906-1141OC

Figure 2

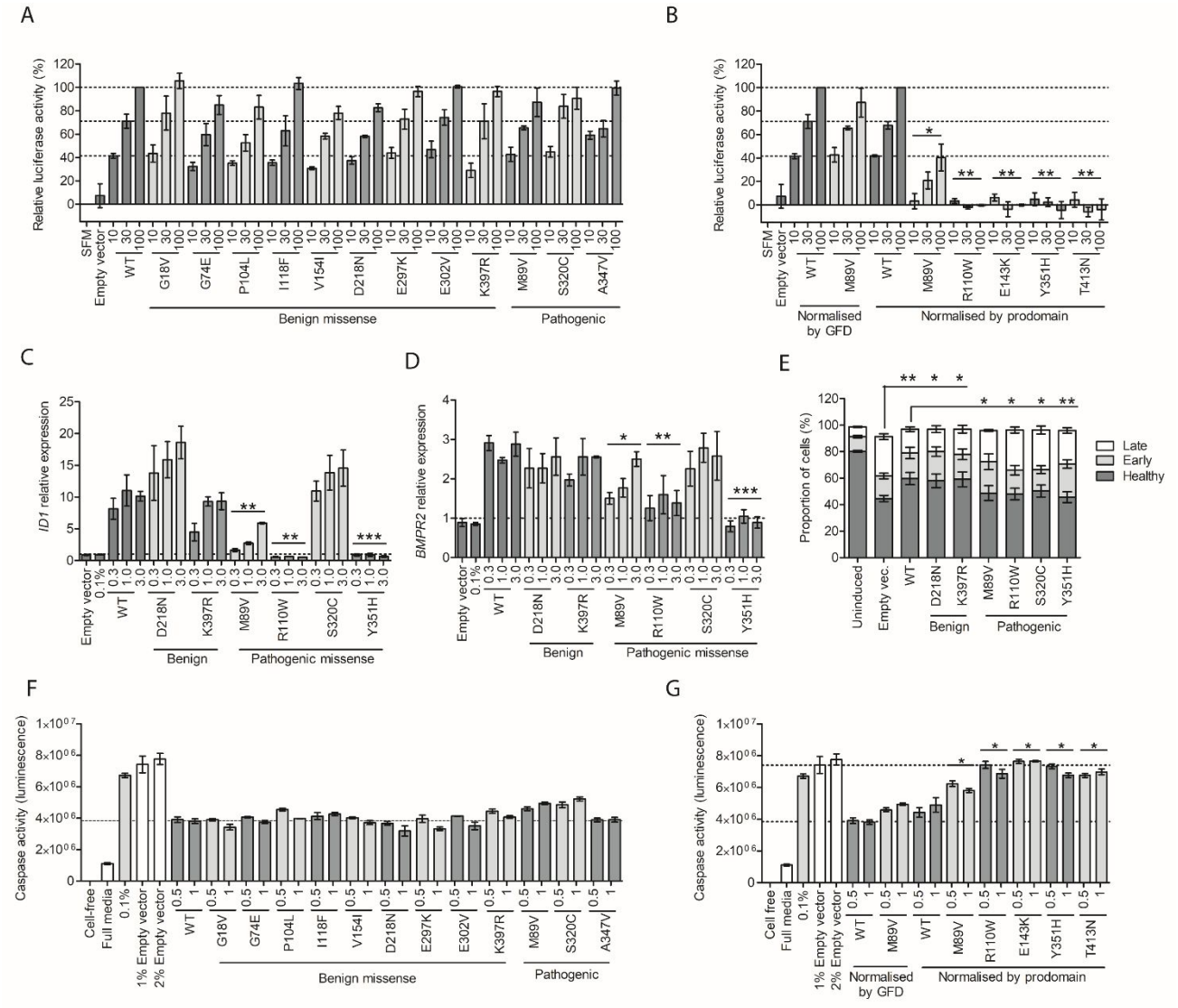

Figure 2: Loss of Activity in Pro:BMP9 Mutants Predicted to be Pathogenic. (a,b) C2C12 cells transfected with human ALK1, BRE-*luciferase* and TK-*Renilla* plasmids were serum-starved followed by treatment with Pro:BMP9 variants (10, 30, 100 pg/ml) for 6h and luciferase assay. The Firefly:*Renilla* luciferase ratios were calculated for each sample and data normalized, with cells treated with 100 pg Pro:BMP9-WT designated as 100%, and SFM-treated cells SFM as 0%. Data are mean ± SEM from three independently generated batches of media. van Elteren test; *P_{adj}<0.05, **P_{adj}<0.01. (c,d) Transcriptional responses of BOECs to Pro:BMP9-WT and variants based on quantification of the prodomains. Cells

were starved in EBM2/0.1% FBS and then treated with Pro:BMP9-WT and variants (0.5, 1.5, 5 ng/ml) for 4 h. The expression of (c) *ID1* and (d) *BMPR2* mRNA were normalized to *B2M* and are expressed as fold change relative to EBM2/0.1% FBS. Data are mean ± SEM from three independently generated batches of media. van Elteren test; $^{**}P_{adj}<0.01$ $^{***}P_{adj}<0.001$. (e) BOECs were treated overnight with 5 ng/ml Pro:BMP9-WT or variants (normalized according to the amount of prodomain) in EBM2/2% FBS followed by induction of apoptosis by addition of TNFα and cycloheximide (TNF/CHX) for 3.5 hours. Cells were stained with Annexin V-FITC and propidium iodide prior to flow cytometry analysis. Cells were assigned as healthy (AV^-/PI^-), early apoptotic (AV^+/PI^-) or late apoptotic/necrotic (AV^+/PI^+). Data are the mean ± SEM from three independently generated batches of media. Paired Dunnett's multiple comparisons test; $^{*}P<0.05$. (f,g) PAECs were starved overnight in EBM2/0.1% FBS to induce apoptosis in the presence of Pro:BMP9-WT or variants (0.5, 1 ng/ml). Each BMP9 treatment was supplemented with conditioned media from HEK-EBNA cells transfected with empty vector to equalize the total volume of conditioned media per well (2% v/v for 1 ng/ml, 1% v/v for 0.5 ng/ml). Apoptosis was measured by Caspase-GLO® 3/7 assays. Data are mean ± SEM from ~~for~~ three independent batches of media. van Elteren test; $^{*}P_{adj}<0.05$

AJRCCM Articles in Press. Published on 29-October-2019 as 10.1164/rccm.201906-1141OC

Figure 3

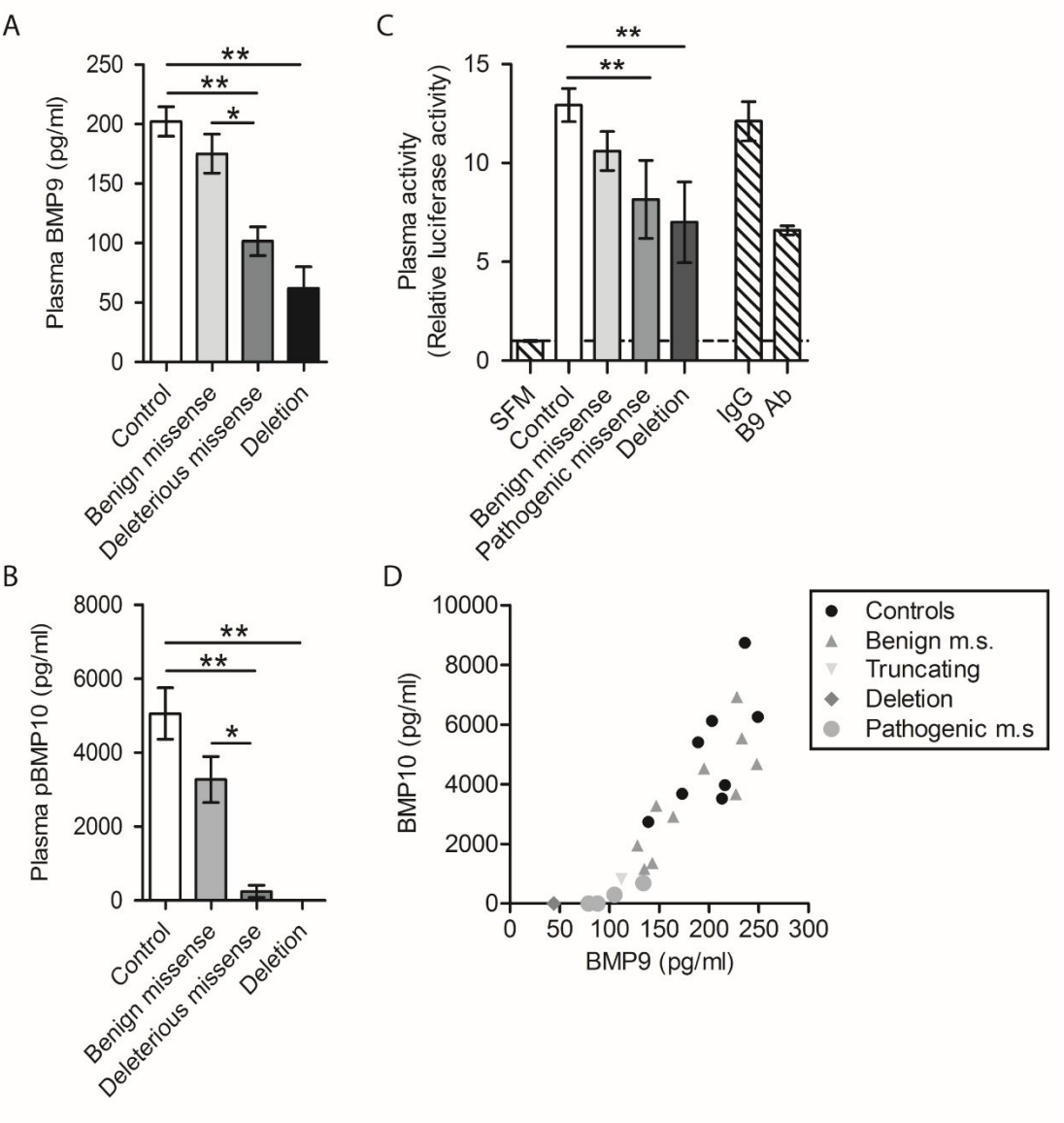

Figure 3: Loss of active BMP9 in PAH patients carrying putatively pathogenic *GDF2* alleles. (a) BMP9 GFD concentration in EDTA-plasma from diseased, *GDF2* heterozygous females and healthy age-matched females was measured by ELISA Data are mean ± SEM; one-way ANOVA; **P*<0.05, ***P*<0.01. (b) HMEC1-BRE cells quiesced in serum free media overnight were treated with 5% plasma for 6 hours before luciferase activity was assessed. Data are mean ± SEM; t-test (c) As for a, but for pBMP10 concentration. (d) The concentration of pBMP10 plotted against the concentration of BMP9 GFD in EDTA-plasma.

Data are mean ± SEM; one-way ANOVA; *P<0.05, **P<0.01. n=8 healthy controls, 11 benign missense, 4 pathogenic missense and 3 deletion (one of which is an early truncation).

AJRCCM Articles in Press. Published on 29-October-2019 as 10.1164/rccm.201906-1141OC

Figure 4

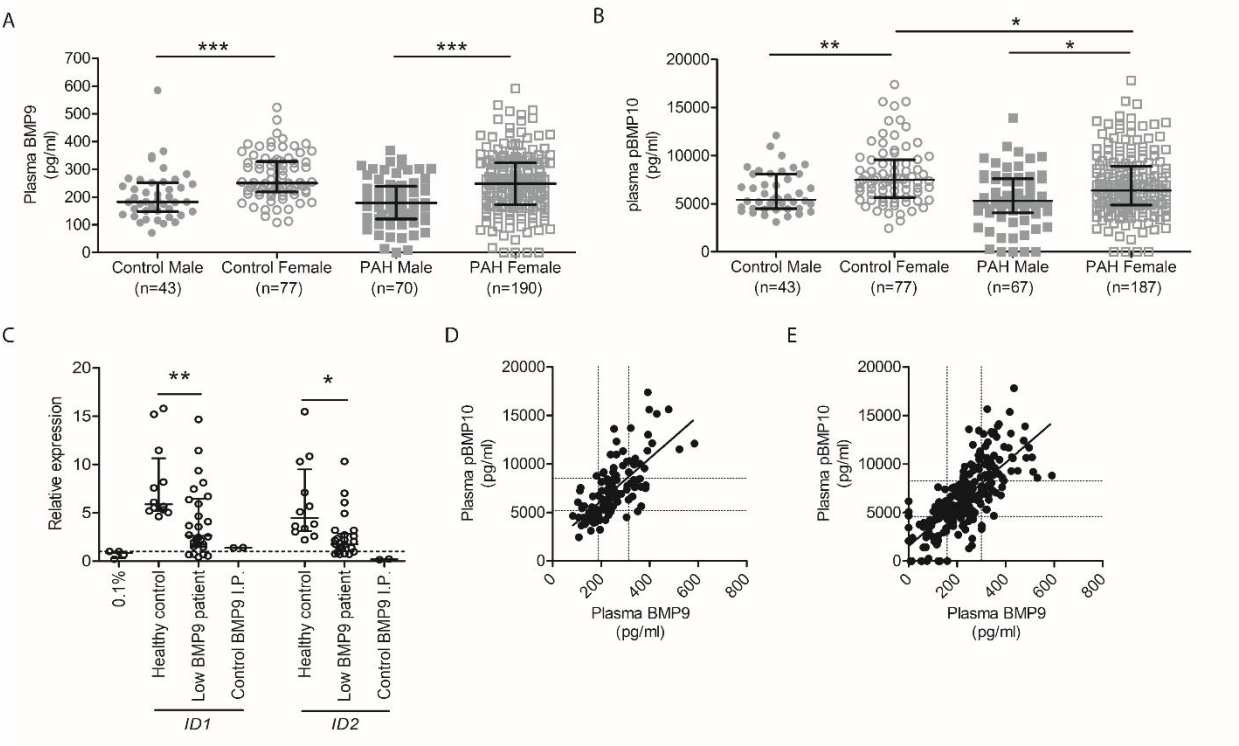

Figure 4: Plasma BMP9 and pBMP10 levels are not reduced in PAH, but a subset of PAH patients exhibit reduced plasma BMP9 and pBMP10 levels. Plasma samples collected from control subjects and PAH patients were assayed for (a) BMP9 and (b) pBMP10. Data are presented as median ± interquartile ranges (Kruskal-Wallis test; ***P*<0.01, ****P*<0.001). (c) hAECs quiesced in 0.1% basal media were incubated with 3% EDTA-plasma for 1 hour. Expression of *ID* mRNA was measured by qPCR and normalized to *B2M* and data expressed as fold-change relative to the EBM2/0.1% FBS control. (mean ± SEM; t-test). (d,e) Plasma BMP9 levels were plotted against plasma pBMP10 levels in (d) control individuals (n=120) and (e) PAH patients (n=187). Dotted lines represent 25% and 75% percentiles. Spearman correlation is shown by a solid regression line.

ONLINE SUPPLEMENTAL MATERIAL

Supplemental Methods

eTable 1: List of clinical case report forms (eCRFs) for data collection

eTable 2 Site directed mutagenesis primers for human ProBMP9 variants

eTable 3: Summary of *GDF2* missense mutations for BMP9 variants assessed functionally in this study.

eTable 4. Clinical phenotypes of *BMP10* mutation carriers.

eTable 5: Clinical characteristics of patients and controls in whom BMP9 and pBMP10 measurements were undertaken.

eTable 6: PAH patients are overrepresented in the lowest 25% of plasma BMP9 and pBMP10 measurements for males and females.

eTable 7: Clinical characteristics at the time of sampling of I/HPAH cases by BMP9 concentration tertiles.

eTable 8: Clinical characteristics at the time of sampling of I/HPAH cases by pBMP10 concentration tertiles.

eFigure 1: Mutations in BMP9

eFigure 2: Efficiency curves for the ELISA analysis of each BMP9 mutant variant.

eFigure 3: Altered glycosylation of the BMP9-D218N variant and impaired furin processing of the BMP9-S320C mutant.

eFigure 4: Dose response of C2C12 myoblasts transfected with or without hALK1.

eFigure 5: Titration of BMP9 variants against BMP9-WT

eFigure 6: Validation of BMP9 GFD ELISA protocol for human plasma.

eFigure 7: Confirmation of high affinity BMP9 responses in the HMEC1-BRE luciferase stable reporter line.

eFigure 8: Validation of pBMP10 ELISA protocol for human plasma.

eFigure 9: BMP9 and pBMP10 levels do not correlate with age for males or females in cases and controls.

eFigure 10: Circulating BMP9 and pBMP10 are physically associated.

eFigure 11: The majority of plasma pBMP10 is unprocessed.

eFigure 12: BMP9 and pBMP10 levels negatively correlate with BMI in PAH cases, but not controls.

eFigure 13: ROC curves for pBMP10 measurements as a predictor of systemic hypertension (HTN) and diabetes mellitus type 2 in I/HPAH patients.

eFigure 14: Kaplan-Meier survival curves for BMP9 and pBMP10 tertiles.

Supplemental references

AJRCCM Articles in Press. Published on 29-October-2019 as 10.1164/rccm.201906-1141OC

Expanded Methods

Case Ascertainment

The 1048 patients who underwent whole genome sequencing comprised the following subgroups: 908 (86.7%) were diagnosed with idiopathic PAH, 58 (5.5%) gave a family history of PAH and 60 (5.7%) gave a history of drug exposure associated with PAH. Twenty two cases (2.1%) held a clinical diagnosis of PVOD/PCH. All patients were clinically phenotyped at the time of diagnosis. The diagnostic criteria for idiopathic or heritable pulmonary arterial hypertension, in accordance with the internationally agreed guidelines were: elevated mean pulmonary artery pressure of >25 mm Hg, with pulmonary capillary wedge pressure <15 mm Hg and pulmonary vascular resistance [PVR] >3 Wood units at rest. Patents with known associated diseases were excluded. The non-PAH patient group (eTable 5) assessed as comparators are described in (1).

Whole Genome Sequencing and Selection of Mutants

The methodologies for high throughput sequencing and analysis of datasets are described in Graf et al 2018 (1). The predicted deleterious impact of amino acid substitutions was analysed *in silico* using the CADD (2), PolyPhen-2 (3), SIFT (4) algorithms. Conservation scores were assessed using the GERP algorithm (5).

Potential PAH-associated pathogenic mutants, confirmed through the *in vitro* analyses undertaken in this study, were defined according to the criteria of: gnomAD frequency <1 in 10000, found in PAH but not other groups and predicted by *in silico* analysis to be damaging. Benign missense variants, confirmed through in vitro analysis in this study, were defined as either (a) those predicted to be benign by in silico analyses or (b) variants which occurred at a frequency of >1/10000 but predicted to be damaging to the structure. Copy number variation analysis for large deletions was assessed as previously described (1).

Clinical phenotyping

Pseudonymised results of routinely performed clinical tests reported in either clinical case notes or electronic medical records (EMR) were stored in web-based *OpenClinica* data capture system (Community edition). Twenty-one electronic Clinical Case Report Forms (eCRFs) (Supplementary eTable 1.) distributed across seven events (Diagnostic, Continuous data, Follow-up, Epidemiology questionnaire, Suspension, Relatives, Unrelated healthy control) were constructed to accommodate routinely available clinical information. To aid data analysis

and improve data quality a number of quality assurance procedures was introduced (automatic and manual data checks, sites monitoring visits). Importantly, diagnosis in all patients was verified based on hemodynamic data, reported comorbidities, pulmonary function tests results, heart, lung and abdominal organs imaging results and clinical blood test data. Portopulmonary hypertension was excluded in accordance with international guidelines.

The date of diagnosis was the starting point to determine follow-up duration between mutation carriers and patients without mutations in known causative genes, date of sampling was a starting point for to determine follow-up duration in patients in whom BMP9 and pBMP10 levels were measured. The cut-off date was assessed via National Health System Digital Spine portal or equivalent local system. Patients lost to follow-up were censored as of the time of the last visit.

ID capture	Echocardiography	Imaging
Demographics	Electrocardiogram	Exercise performance
Functional class	Lung function	Body system
Clinical features by history	Associated Diseases	Drug treatment history (PAH)
Clinical features by examination	Clinical blood tests	Drug treatment history (other)
Risk factors	Survival	Family history
Hemodynamics	Arterial blood gasses	Epidemiology questionnaire

eTable 1: List of clinical case report forms (eCRFs) for data collection

Statistical analyses of association of *GDF2* mutations with clinical phenotypes

The hypothesis tested was to analyse whether PAH patients harboring pathogenic *GDF2* mutations exhibited a specific phenotype compared to either patients with BMPR2 mutations or patients without a mutation in a known PAH gene. Baseline characteristics of the PAH cohort were expressed as numbers and percentages for categorical variables, and median (interquartile range) for continuous variables according to data distribution. Between groups comparisons were performed using chi-squared test or Kruskal-Wallis rank sum test. The association of mutation status with the risk of death was assessed using Cox proportional hazards regression models. All model assumptions were checked and met. The Kaplan-Meier method was used to estimate overall survival and survival according to mutation status, log-rank test was used for comparisons**.**

Statistical analyses of association of plasma BMP9 and pBMP10 levels with clinical phenotypes

The hypothesis tested was to analyse if measured plasma levels of BMP9 or pBMP10 in PAH patients were associated with other clinical indices of either PAH or co-morbidities. BMP9 and pBMP10 were measured in specifically in patients diagnosed with IPAH or HPAH, with exclusion of other Group1 diagnoses and Group 2-

AJRCCM Articles in Press. Published on 29-October-2019 as 10.1164/rccm.201906-1141OC

5 diagnoses. Clinical information from the time of sampling was prospectively collected for PAH patients. Categorical data were expressed as numbers and percentages and mean ± standard deviation or median (interquartile range) for continuous variables as per data distribution. Normality assumptions were tested using the Shapiro-Wilk test. Comparisons between and within groups were performed using parametric and nonparametric tests according to data distribution.

The association of BMP9 and pBMP10 levels with risk of death was assessed using Cox proportional hazard regression models. Model assumptions were assessed and satisfied. Overall survival and transplant-free survival were calculated from diagnosis and sampling. Where a significant p-value was obtained the analysis was adjusted for confounders (sex and age at sampling or age at diagnosis). Ligand levels (dependent variable) were expressed as a continuous variable, tertiles and binary variable above and below LOQ.

Binary logistic regression models were fitted to describe the relationship between a binary outcome (diagnosis of diabetes mellitus type 2 (DM type 2) and systemic hypertension (HTN)) and BMP9 and pBMP10 levels. ROC curves based on a fit of a logistic regression models for both comorbidities were subsequently constructed.

Cell culture

HEK-EBNA cells (ATCC; Manassas, VA) and C2C12 mouse myoblasts (A gift of Professor C. Shanahan, King's College London, UK) were grown in Dulbecco's Modified Eagle Medium (DMEM; Gibco 41965) with 10% foetal bovine serum (FBS; Invitrogen A384000) and antibiotic-antimycotic (Invitrogen 15420). Pulmonary artery endothelial cells (PAECs; Lonza), human aortic endothelial cells (hAECs; Lonza) and Blood outgrowth endothelial cells (BOECs) isolated from control subjects (6) were maintained in EBM2 basal media (Lonza CC-3156) and EGM-2 Singlequot supplements (Lonza CC-4176). For hAECs, 5% FBS was used. For BOECs, 10% FBS was used with the heparin omitted.

Human microvascular endothelial cells (HMEC-1; LGC Standards) stably expressing the BRE-luciferase reporter (HMEC-BRE) were grown in MDCB-131 media (Gibco 10372019) supplemented with 10% FBS, 10 mM L-Glutamine (Invitrogen 25030-032), 1 mg/ml Hydrocortisone (Sigma H0888), 10 ng/ml EGF (Sigma E9644) and antibiotic/antimycotic. In brief, cells were transfected with linearized pGL3-$(BRE)_2$-Luciferase (A kind gift from Professor Peter ten Dijke, Leiden University Medical Center, Netherlands)(7) and pSelect-puro (Invivogen) followed by selection with puromycin for 10-days. Puromycin-resistant cells were then expanded and high affinity BMP9 responsiveness confirmed. For treatments, cells were starved overnight in serum-free

MDCB-131, followed by incubation with plasma samples for 6 hours. Cells were lysed with One-Glo reagent (Promega) and luciferase measures in a Promega GloMax® Multi+ luminometer.

BMP9 ELISA

The BMP9 ELISA detected the BMP9 GFD and Pro:BMP9 with equivalence, and did not cross-react with the BMP10 GFD or Pro:BMP10 (eFigure S6a). As suggested below, this assay is unlikely to detect *ProBMP9*.

Spike recovery testing was assessed by preparing serial dilutions of pBMP9-wt (2500 pg/ml, 5000 pg/ml and 10000 pg/ml) or BMP9-GFD (2500 pg/ml and 5000 pg/ml) in plasma. BMP9 immunoreactivity was measured in 1 µl, 5 µl, 10 µl, 15 µl and 25 µl of each serial dilution made to 100 µl with PBS/1% BSA. Four supplements were tested: (1) 0.2% GS, (2) 0.2% GS plus 0.5% Triton X-100, (3) 0.2% GS + 4.5 mM EDTA and (4) 0.2% GS plus 0.5% Triton X-100 and 4.5 mM EDTA. Of these, Triton X-100 and GS, to reduce plasma matrix interactions, increased the recovery of exogenous BMP9, whereas EDTA had no additive effect (eFigure S7b-g).

For testing of the recovery of endogenous BMP9, immunoreactivity was measured in 5 µl, 10 µl, 15 µl, 25 µl, 50 µl and 100 µl of plasma, diluted with PBS/1% BSA to a total of 100 µl. To test the effect of 0.2% GS plus 0.5% Triton X-100, a 21X concentrated mix was added to samples. Although higher recovery efficiency was achieved with 15 µl and 10 µl plasma (eFigure S7b-g), 25 µl was the lowest volume that permitted reliable measurement of endogenous BMP9 (eFigure S7h). The optimized ELISA protocol did not detect any non-specific binding in samples which had undergone BMP9 immunoprecipitation (eFigure S7h). ELISA quantifications of Pro:BMP9-WT and pBMP9-S320C compared to western blotting and activity data, suggested that this ELISA only detected active Pro:BMP9 and probably does not detect *ProBMP9*.

The optimized protocol was performed as follows:

For plasma BMP9 measurements, high binding 96-well ELISA plates (Greiner 655061) were coated with 0.5 µg/well anti-human BMP9 (R&D Systems MAB3209) in PBS (ThermoFisher BP2438), and incubated overnight at 4°C in a humidified chamber. Plates were washed with PBS containing 0.05% Tween 20 (PBS-T), followed by blocking with 1% (w/v) bovine serum albumin (BSA, ThermoFisher 12737119) in PBS (PBS/1% BSA) for 2 hours at RT. Plasma samples (25µl) were premixed with 75µl PBS/1% BSA containing 0.667% Triton X-100 and 0.267% GS to give final concentrations of 0.5% Triton X-100 and 0.2% GS. Recombinant human BMP9 standards (4.88-5000 pg/ml) were prepared in the same final concentrations of additives. After washing, 0.04 µg/well of anti-human BMP9 detection antibody (R&D Systems BAF3209) was added in

AJRCCM Articles in Press. Published on 29-October-2019 as 10.1164/rccm.201906-1141OC

PBS/1% BSA containing 0.2% GS. After washing, ExtrAvidin(r)-Alkaline phosphatase (Sigma E2636) diluted 1:400 in PBS/1% BSA was added. The ELISA was developed with 1mg/ml 4-Nitrophenyl phosphate disodium salt hexahydrate (Sigma N2640) in 1 M Diethanolamine / 0.5 mM $MgCl_2$, pH9.8 and absorbance measured at 405 nm. Unknown values were extrapolated from the standard curve using a 4-parameter log curve fit. All values are presented as the concentration of the BMP9-GFD. Technical duplicates of each sample were assayed, and the mean of each duplicate was used as a single data point in statistical analyses.

For measurement of BMP9 in conditioned media, the above assay was used with 0.2 µg/well of MAB3209 and without supplements. Serial dilutions of conditioned media samples were assayed. Detection efficiency curves were plotted by using the average estimated neat concentration to infer the concentration after dilution, and the slope of these curves was compared to that of the BMP9-GFD standard.

pBMP10 ELISA

This ELISA detects Pro:BMP10 and *ProBMP10*, therefore we refer to 'pBMP10'. This ELISA does not detect the BMP10 GFD alone, Pro:BMP9 nor BMP9 GFD (eFigure 8a, 11a).

Spike recovery testing was assessed by preparing serial dilutions of Pro:BMP10 (25ng/ml, 50ng/ml and 100ng/ml) in control plasma followed by measurement of Pro:BMP10 immunoreactivity in 1 µl, 5 µl, 10 µl, 15 µl and 25 µl of each dilution. Diluent composition and plasma loading volumes were assessed as for the BMP9 ELISA (eFigure 8).

The optimized protocol was performed as follows:

For plasma pBMP10 measurements, plates were coated with 0.5 µg/well of anti-human BMP10 (MAB2926; R&D Systems) and blocked as above. Plasma samples(30µl) were premixed with 70µl PBS/1% BSA containing 0.714% Triton X-100, 0.286% GS and 6.42mM EDTA (final = 0.5% Triton X-100, 0.2% GS and 4.5 mM EDTA). Dilutions of the furin-cleaved purified Pro:BMP10 standard (97.65-100000pg/ml GFD equivalent), produced as described previously (8), were prepared to give the same final concentrations of additives. After washing, anti-human BMP10 propeptide (0.04 µg/well, R&D Systems BAF3956) in 1% BSA, 0.2% goat serum was added. Assays were then processed as described for BMP9. All data are presented as the concentration of the GFD component.

BMP10 GFD ELISA

This ELISA detects Pro:BMP10 and BMP10 GFD, but not *ProBMP10* (eFigure 11b). Spike recovery testing was performed by serially diluting Pro:BMP10 (3-50 pg/ml) in control plasma followed by measurement of immunoreactivity. Since levels in control plasma were so low, samples were diluted in BioRad ELISA diluent (BUF037A) was used to dilute samples, which slightly improved recovery efficiency.

The protocol was performed as follows:

Capture and detection antibodies were from a commercially available kit (R&D systems DY2926-05) and used according to the manufacturer's instructions. Plasma samples (30µl) were premixed with 70µl BUF037A containing 0.714% Triton X-100, 0.286% GS and 6.42mM EDTA (final = 0.5% Triton X-100, 0.2% GS and 4.5 mM EDTA). Dilutions of the furin-cleaved purified Pro:BMP10 standard (97.65-100000pg/ml GFD equivalent), produced as described previously (9) were prepared to give the same final concentrations of additives. Assays were then processed as described for BMP9. All data are presented as the concentration of the GFD component.

Plasma samples

Control EDTA plasma samples (n=120) were collected at Imperial College London from healthy volunteers with no known history of pulmonary arterial hypertension. Samples from PAH patients (n=260) were collected via the UK National Cohort Study of IPAH and HPAH Biobank. Patients were selected according to a confirmed diagnosis of IPAH or HPAH, with exclusion of patients with pulmonary veno-occlusive disease, pulmonary capillary hemangiomatosis or if pulmonary capillary wedge pressure was >15. BMP9 levels were measured in 260 PAH samples, but pBMP10 measured in 254 of these samples due to insufficient volume of 6 samples. Whole genome sequencing had been undertaken on all but 2 of these patients, both of whom had normal circulating BMP9 and pBMP10 levels.

Immunoprecipitation

Protein G conjugated beads (15 µl per sample, ThermoFisher 10004D) were incubated with 20 µl of MAB3209 (anti-BMP9), MAB2926 (anti-BMP10) or ALK1-Fc (R&D systems 370-AL) in PBS for 1 hour with rotating. Beads were washed and incubated with 200 µl of plasma overnight at room-temperature with rotating. Beads were then separated with a magnet.

AJRCCM Articles in Press. Published on 29-October-2019 as 10.1164/rccm.201906-1141OC

HMEC-1-BRE luciferase assay

HMEC-1 cells stably expressing a BMP-Smad response element luciferase reporter (HMEC1-BRE) were quiesced in serum free MDCB-131 media overnight, then treated with 5% plasma for 6 hours followed by lysis and analysis with One-Glo reagent. Each sample was measured in triplicate, and the mean of each triplicate was used as a single data point.

***In Vitro* production and testing of BMP9 variants**

Site-Directed Mutagenesis

The cloning of the pCEP4-ProBMP9 wild-type (WT) expression vector used for site-directed mutagenesis (SDM) has been described previously (9). SDM was carried using PfuTurbo (Agilent 600250) using the mutagenesis primers detailed in eTable 1. Sequences were verified by Sanger sequencing (Source Bioscience).

eTable 2: Site directed mutagenesis primers for human ProBMP9 variants

Mutation	Primer Sequences	
p.Gly18Val	For:	5'-CTGCTGGCTgtcTCCCTACAGGGGAAG-3'
	Rev:	5'-CCCTGTAGGGAgacAGCCAGCAGGGAC-3'
p.Gly74Glu	For:	5'-AGCCTTAACCTGAGTgagGTCCCTTCGCA-3'
	Rev:	5'-TGCGAAGGGACctcACTCAGGTTAAGGC-3'
p.Met89Val	For:	5'-CCGCCGCAGTACgtgATTGACCTGTACAAC-3'
	Rev:	5'-GTACAGGTCAATcacGTACTGCGGCGGCT-3'
p.Prol104Leu	For:	5'-AAGTCGACTACGctaGCGTCCAACATTGTG-3'
	Rev:	5'-GCACAATGTTGGACGCtagCGTAGTCGACTTA-3'
p.Arg110Trp	For:	5'-CGTCCAACATTGTGtggAGCTTCAGCAT-3'
	Rev:	5'-ATGCTGAAGCTccaCACAATGTTGGAC-3'
p.Ile118Phe	For:	5'-TGGAAGATGCCttcTCCATAACTGCCACA-3'
	Rev:	5'-GCAGTTATGGAgaaGGCATCTTCCATGCT-3'
p.Glu143Lys	For:	5'-CCATTCCTAGGCATaagCAGATCACCAGA-3'
	Rev:	5'-GCTCTGGTGATCTGcttATGCCTAGGAATG-3'
p.Val154Ile	For:	5'-TGAGCTCCGACTCTATatcTCCTGTCAAAATCACG-3'
	Rev:	5'-TTTTGACAGGAgatATAGAGTCGGAGCTCAG-3'
p.Asp218Asn	For:	5'-GGGTCCGGTCCaacTCCACCAAGAGCA-3'
	Rev:	5'-TTTGCTCTTGGTGGAgttGGACCGGACCC-3'
p.Glu297Lys	For:	5'-TCCACAGAGGCAGGTaagAGCAGTCACGA-3'
	Rev:	5'-CTCGTGACTGCTcttACCTGCCTCTGTGGA-3'
p.Glu302Val	For:	5'-GAGCAGTCACGAGgtgGACACGGATGGC-3'
	Rev:	5'-CCATCCGTGTCcacCTCGTGACTGCTCT-3'
p.Ser320Cys	For:	5'-GGAAAAGGtgcGCCGGGGCTGGCAGCCACT-3'
	Rev:	5'-TGCCAGCCCCGGCgcaCCTTTTCCGCCT-3'
p.Ala347Val	For:	5'-AGCTGGATCATTgtaCCCAAGGAGTATGAA-3'
	Rev:	5'- GCTTCATACTCCTTGGGtacAATGATCCAG-3'
p.Tyr351His	For:	5'-ATTGCACCCAAGGAGcatGAAGCCTACGAGT-3'
	Rev:	5'-CTCGTAGGCTTCatgCTCCTTGGGTGCAAT-3'
p.Lys397Arg	For:	5'-CTGTGTGCCCACCagaCTGAGCCCCAT-3'
	Rev:	5'-AGATGGGGCTCAGtctGGTGGGCACACA-3'
p.Thr413Asn	For:	5'-ATGGGGGTGCCCaacCTCAAGTACCATTA-3'
	Rev:	5'-TGGTACTTGAGgttGGGCACCCCCATGTC-3'

Production of non-processable *ProBMP10*

A non-processable *ProBMP10* variant was also produced by mutagenizing the pCEP4-ProBMP10 WT expression vector (8). A Q5 site-directed mutagenesis kit (NEB E0554S) was used with For: 5'-CTCCACTGCCgcAATCAGAAGG-3' and Rev: 5'- TCATAGATGATGTTTGATCT-3' primers. The mutation results in an amino-acid change within the *ProBMP10* furin recognition sequence, R313A. Uncleaved dimeric *ProBMP10* was purified as described (8).

Production of BMP9 Wild Type and Variant Proteins

Plasmids were transfected into HEK-EBNA cells using polyethylenimine (Polysciences 23966-2) in DMEM containing 5% FBS. Cells were changed into serum-free CDCHO expression medium (Gibco 10743029) the following day. On day 6, conditioned media were harvested and cleared by centrifugation, with aliquots then stored at -80^{o}C. Cell lysates were snap-frozen in SDS-buffer (125 mM Tris pH 7.4, 10% glycerol, 2% SDS) supplemented with protease/phosphatase inhibitor (Sigma 11836170001), followed by sonication. For each variant, three batches of expression media were generated on separate occasions to ensure reproducibility of our observations.

Immunoblotting

Lysates or culture supernatants were mixed with reducing or non-reducing loading buffer to give a 1X loading buffer concentration (62.5mM Tris.HCl pH6.8, 2% SDS, 10% glycerol, 0.0025% bromophenol blue, ± 12.5% β-mercaptoethanol) and heated at 98°C for 5 min. Samples were immunoblotted and probed for the growth factor domain with MAB3209 (1:1000; R&D Systems) for non-reduced samples or sc-514211 (1:1000; Santa Cruz Biotechnology) for reduced samples. The prodomain was blotted using AF3879 (1:2500; R&D Systems). Lysate blots were re-probed with an antibody toward β-actin (Sigma A5441, clone AC-15). Densitometry was performed using FIJI Is Just ImageJ software.

C2C12-ALK1-BRE-luciferase assay

BMP9 signaling activity was measured as previously described (8). C2C12 cells were seeded in 24 well plates and placed in Opti-MEM-1 (31985 Invitrogen). Cells were transfected with pcDNA3-hALK1 (kindly provided by Professor Richard C. Trembath, King's College London, UK) or pcDNA3 empty vector, pGL3-$(BRE)_2$-Luciferase and pRL-TK (Promega E2241) using Lipofectamine 2000 (ThermoFisher 116680). After 4 h, the

AJRCCM Articles in Press. Published on 29-October-2019 as 10.1164/rccm.201906-1141OC

transfection mixes were removed and growth media added to the cells. After 24 h cells were washed in serum-free DMEM (SFM) overnight.

Cells were treated in SFM containing pBMP9-WT or variants for 6 h. Technical triplicates of each sample were assayed, and the mean of each triplicate was used as a single data point in statistical analyses. The amount of conditioned media used was normalized to 10, 30 or 100 pg/ml based on ELISA quantification of the amount of BMP9 present. For pathogenic variants where the growth factor domain was highly unstable, quantification was based on western blotting of the prodomain. For the empty vector control, a larger volume of conditioned media was used than for the pBMP9 mutant with the lowest concentration. Cells were lysed and assayed for Firefly and *Renilla* luciferase activities of using the Dual-Glo Luciferase assay system (Promega E2920) on a GloMax luminometer (Promega). The BRE-Luciferase activity was normalized to the *Renilla* Luciferase activity for each sample. The data from each plate were then normalized such that the negative control (SFM) was defined as 0% and the positive control (SFM plus 100 pg/ml pBMP9-WT) was assigned a value of 100%.

Deglycosylation

Protein in conditioned media was deglycosylated using PNGase F according to the manufacturer's instructions (NEB P0704). Approximately 15ng of BMP9-GFD, calculated by ELISA, was deglycosylated and then fractionated by SDS-PAGE.

Transcriptional responses

For assessing the transcriptional responses of BOECs to Pro:BMP9-WT and variants, or hAECs to patient plasma samples, cells were starved in EBM2 containing 0.1% FBS (EBM2/0.1% FBS) and then treated with Pro:BMP9-WT and variants (0.5, 1.5, 5 ng/ml) for 4 hours, or 1% plasma for 1 hour, followed by lysis for RNA extraction. Total RNA was extracted using the RNeasy Mini Kit with on-column DNAse digestion (Qiagen). cDNA was prepared using a High Capacity Reverse Transcriptase kit (Applied Biosystems). All qPCR reactions were prepared with SYBRGreen Jumpstart Taq Readymix (Sigma-Aldrich), ROX reference dye (Invitrogen). Custom sense and anti-sense primers for human were: *B2M:* Forward: 5'-CTCGCGCTACTCTCTCTTTCT-3', Reverse: 5'-CATTCTCTGCTGGATGACGTG-3'; *ID1:* Forward: 5'-CGAAGTTGGAACCCCGGG-3', Reverse: 5'-CAGGAACGCATGCCGCCTCG-3'; *BMPR2:* Forward: 5'CAAATCTGTGAGCCCAACAGTCAA-3', Reverse: 5'-GAGGAAGAATAATCTGGATAAGGACCAAT-3'*B2M, BMPR2, ID1,* were all designed using PrimerBlast (NCBI) (eTable 2). Reactions were amplified on a

StepOnePlus Real-Time PCR system (Applied Biosystems). Relative expression of each target gene was calculated using the comparative $2^{-(\Delta\Delta Ct)}$ method normalized to *B2M.*

Annexin V/PI Apoptosis Assay

Apoptosis inhibition in response to BMP9 was measured as previously described (10). BOECs grown in 6-well plates were incubated in EBM2 with 2% FBS (EBM2/2% FBS) overnight alone, or with addition of diluted HEK-EBNA conditioned media with 3 ng/ml of BMP9-GFD as calculated by ELISA. After 16 hrs, cycloheximide (CHX, Sigma C7698) and TNFα (TNF, R&D Systems 210-TA) were added to the wells to final concentrations of 50 µg/ml CHX and 3 ng/ml TNF. After 3-4 hrs, cells were trypsinized and transferred into ice-cold PBS. Cells were then stained with the Annexin V/PI apoptosis detection kit (BD biosciences 556547) according to the manufacturer's instructions. Staining was analysed with an Accuri flow-cytometer (BD biosciences). Data were exported to FlowJo (version 10) for analysis.

Caspase- GLO® 3/7 Assay

PAECs were grown in 48 well plates. They were then washed and placed into 200 µl EBM2 with 0.1% FBS, or EGM2 as a negative control. The EBM2 was supplemented with a mix of conditioned media from HEK-EBNA cells transfected with empty vector and variant BMP9 expression vectors such that the cells were exposed to 1 ng/ml BMP9 and 2% v/v conditioned media, or 0.5 ng/ml BMP9 and 1% v/v conditioned media. Technical triplicates of each sample were assayed, and the mean of each triplicate was used as a single datapoint in statistical analyses. After overnight treatment, 100 µl of Caspase-GLO® 3/7 reagent (Promega G8091) was added and samples analysed on a Promega GloMax® Multi+ luminometer.

Statistical analysis of *in vitro* data

The hypothesis tested was that some *GDF2* mutants may be functionally impaired or poorly secreted. Therefore, we generated three independent batches of conditioned media, each batch produced on a different day with a fresh transfection. All *in vitro* experiments were repeated three times, using a different batch for each repeat, and statistically compared using matched/paired tests.

For the C2C12-ALK1-BRE-luciferase, transcriptional response and CaspaseGlo assays, a stratified van Elteren test was carried out to compare the response of variant BMP9 to WT BMP9. *P* values were adjusted to account for multiple testing with the Bonferroni method. For measurements of BMP9 secretion into conditioned media,

AJRCCM Articles in Press. Published on 29-October-2019 as 10.1164/rccm.201906-1141OC

and the ratio of prodomain to growth-factor domain, a paired Dunnett's multiple comparisons test was used to compare the secretion of BMP9 variants to WT BMP9. For analysis of Annexin V/PI apoptosis data, a Freidman test was applied with a paired Dunnett's multiple comparisons test. For analysis of plasma BMP9 measurements in ELISA validation and immunprecipitation studies, data were analysed by one-way or two-way ANOVA. Data analyses were performed using GraphPad Prism 5 or R and results are shown as mean±SEM.

			Disease Groups																	
	hgvsc	**HGVSp**	**PAH**	**BPD**	**CSVD**	**GEL**	**HCM**	**ICP**	**NPD**	**MPMT**	**PID**	**SMD**	**SPEED**	**SRNS**	**Sum**	**gnomAD frequency**	**CADD**	**SIFT**	**PolyPhen-2**	**GERP**
PAH Pathogenic Missense	**c.265A>G**	**p.Met89Val (M89V)**	**1**	**0**	**0**	**0**	**0**	**0**	**0**	**0**	**0**	**0**	**0**	**0**	**1**	0	**24.8**	**D(0)**	**Pr(0.999)**	**5.37**
	c.328C>T	**p.Arg110Trp (R110W)**	**1**	**0**	**0**	**0**	**0**	**0**	**0**	**0**	**0**	**0**	**0**	**0**	**1**	0	**35**	**D(0)**	**Pr(1)**	**4.35**
	c.347A>T	**p.Asp116Val (D116V)**	**1**	**0**	**0**	**0**	**0**	**0**	**0**	**0**	**0**	**0**	**0**	**0**	**1**	0	**24.4**	**D(0.01)**	**Po(0.933)**	**4.41**
	c.427G>A	**p.Glu143Lys (E143K)**	**1**	**0**	**0**	**0**	**0**	**0**	**0**	**0**	**0**	**0**	**0**	**0**	**1**	0	**28**	**D(0)**	**Pr(1)**	**4.65**
	c.958A>T	**p.Ser320Cys (S320C)**	**1**	**0**	**0**	**0**	**0**	**0**	**0**	**0**	**0**	**0**	**0**	**0**	**1**	3.98E-06	**23.3**	**D(0.01)**	**Pr(1)**	**5.46**
	c.1040C>T	**p.Ala347Val (A347V)**	**1**	**0**	**0**	**0**	**0**	**0**	**0**	**0**	**0**	**0**	**0**	**0**	**1**	3.98E-06	**23.9**	**D(0)**	**Pr(0.984)**	**5.63**
	c.1051T>C	**p.Tyr351His (Y351H)**	**2**	**0**	**0**	**0**	**0**	**0**	**0**	**0**	**1**	**0**	**0**	**0**	**3**	1.59E-05	**23.8**	**D(0)**	**Pr(1)**	**5.63**
	c.1238C>A	**p.Thr413Asn (T413N)**	**1**	**0**	**0**	**0**	**0**	**0**	**0**	**0**	**0**	**0**	**0**	**0**	**1**	4.49E-06	**26.3**	**D(0)**	**Pr(1)**	**5.52**
Benign Missense	*c.53G>T*	*p.Gly18Val (G18V)*	*1*	*0*	*0*	*0*	*0*	*0*	*0*	*0*	*0*	*0*	*0*	*0*	*1*	*0*	*18.47*	*T(0.19)*	*B(0.036)*	*4.78*
	c.221G>A	*p.Gly74Glu (G74E)*	*1*	*1*	*1*	*3*	*0*	*0*	0	*0*	*0*	*1*	*0*	*0*	*7*	*2.12E-04*	*15.93*	*D(0.04)*	*B(0.395)*	*4.47*
	c.244A>G	*p.Arg82Gly R82G)*	*2*	*0*	*0*	*0*	*0*	*0*	*0*	*0*	*3*	*0*	*0*	*0*	*5*	*1.11E-04*	*24.2*	*D(0)*	*Po(0.863)*	*0.39*
	c.311C>T	*p.Pro104Leu (P104L)*	*1*	*0*	*0*	*0*	*0*	*0*	*0*	*0*	*0*	*0*	*1*	*0*	*2*	*3.19E-05*	*28.8*	*D(0)*	*Pr(1)*	*5.37*
	c.352A>T	*p.Ile118Phe (I118F)*	*2*	*0*	*0*	*0*	*0*	*1*	*0*	*0*	*0*	*0*	*0*	*1*	*4*	*1.11E-03*	*0.006*	*T(0.61)*	*B(0.369)*	*-5.22*
	c.460G>A	*p.Val154Ile (V154I)*	*1*	*0*	*0*	*0*	*0*	*0*	*0*	*0*	*0*	*0*	*0*	*0*	*1*	*3.98E-06*	*8.365*	*T(0.54)*	*B(0.011)*	*-2.13*
	c.652G>A	*p.Asp218Asn (D218N)*	*3*	*4*	*2*	*8*	*0*	*4*	*0*	*0*	*0*	*7*	*7*	*2*	*37*	*2.51E-03*	*24.4*	*D(0.04)*	*Pr(0.999)*	*5.59*
	c.871G>A	*p.Gly291Ser (G291S)*	*1*	*0*	*0*	*2*	*1*	*0*	*0*	*0*	*0*	*0*	*0*	*0*	*4*	*7.07E-05*	*0.002*	*T(0.53)*	*B(0.007)*	*-7.65*
	c.889G>A	*p.Glu297Lys (E297K)*	*1*	*0*	*0*	*0*	*0*	*0*	*0*	*0*	*0*	*0*	*0*	*0*	*1*	*1.59E-05*	*5.909*	*T(0.13)*	*B(0.005)*	*4.11*
	c.905A>T	*p.Glu302Val (E302V)*	*2*	*0*	*0*	*0*	*0*	*0*	*0*	*0*	*0*	*0*	*0*	*0*	*2*	*0*	*5.967*	*T(0.18)*	*Po(0.698)*	*1.47*
	c.911C>T	*p.Thr304Met (T304M)*	*1*	*0*	*0*	*0*	*2*	*0*	*3*	*1*	*0*	*0*	*3*	*2*	*14*	*1.67E-03*	*0.007*	*T(0.12)*	*B(0036)*	*-5.33*
	c.997C>T	*p.Arg333Trp (R333W)*	*1*	*0*	*0*	*0*	*0*	*0*	*0*	*0*	*2*	*0*	*0*	*0*	*3*	*4.07E-04*	*6.425*	*T(0.08)*	*B(0.024)*	*-0.216*
	c.1190A>G	*p.Lys397Arg (K397R)*	*0*	*0*	*0*	*1*	*0*	*0*	*0*	*0*	*0*	*0*	*0*	*0*	*1*	*2.50E-04*	*25.8*	*D(0.01)*	*Pr(0.997)*	*5.52*

eTable 3: Summary of *GDF2* missense mutations for BMP9 variants assessed functionally in this study.

Bold - variants defined in this study as PAH pathogenic missense, Italics – variants defined as benign missense. ***Disease Groups***: PAH - idiopathic and heritable pulmonary arterial hypertension; BPD - bleeding, thrombotic and platelet disorders, CSVD - cerebral small vessel disease, GEL – 100,000 Genomes Study UK, HCM – hypertrophic cardiomyopathy, ICP - intrahepatic cholecystis of pregnancy, NPD – neuropathic pain disorders, MPMT – multiple primary malignant tumours, PID - primary immune disorders, SMD - stem cell and myeloid disorders, SPEED - specialist pathology: evaluating exomes in diagnostics, SRNS - steroid resistant nephrotic syndrome, ***SIFT:*** D – Deleterious, T – Tolerated. ***PolyPhen-2:*** Pr – probably damaging, Po – possibly damaging, B = benign. Dark grey cell for D218N: 3 homozygote patients identified.

AJRCCM Articles in Press. Published on 29-October-2019 as 10.1164/rccm.201906-1141OC

Variable	**E001250**	**E010850**
	Gene changes	
Nucleotide change	c.1082C>A	c.1057C>T
Protein change	p.Ala361Glu (A361E)	p.Arg353Cys (R353C)
Consequence	Missense variant	Missense variant
CADD	25.7	28.2
SIFT	deleterious	deleterious
PolyPhen-2	Probably damaging	Probably damaging
GERP	6.07	6.07
	Demographics and functional status	
Age at diagnosis	72	28
Sex	male	female
Ethnic category	White & Black Caribbean	Other White
Genetic race	African	Other
WHO class	3	4
6MWD [m]	340	215
	Hemodynamics	
mRAP [mmHg]	5	6
mPAP [mmHg]	30	71
PAWP [mmHg]	8	8
PVR [mmHg]	16.5	18
CO [L/min]	1.33	3.50
	Clinical blood tests	
Hb [g/l]	106	
RDW [%]	17.6	
WBC x10e9/l	2.7	
Platelets x10e9/l	168	
Creatinine [µmol/l]	129	
BNP [ng/]l	171.8	220.0
ALP [IU/l]	92	
Albumin [g/l]	40	
ALT [IU/l]	26	
AST [IU/l]	27	
Bilirubin [µmol/l]	10	
Total protein [g/l]	74	
Cholesterol [mmol/l]	4.6	
HDL [mmol/l]	1.16	
LDL [mmol/l]	2.93	
TG [mmol/l]	1.12	
	Lung function tests	
FEV1 [% pred.]	82	67
FVC [% pred.]	82	65
FEV1/FVC	0.76	
KCO [% pred.]	92	
	Comorbidities	
	Systemic hypertension with LV hypertrophy, obstructive sleep apnoea, mild chronic kidney disease with renal cysts, cataract, benign prostatic enlargement	Diabetes mellitus type 2, systemic hypertension
	Family history	
Family members with PAH	No	No

eTable 4. Clinical phenotypes of *BMP10* mutation carriers.

WHO FC class – World Health Organization functional class; 6MWT – 6 minute walk test; mRAP – mean right atrial pressure; mPAP – mean pulmonary arterial pressure; PAWP - pulmonary artery wedge pressure; PVR – pulmonary vascular resistance; CO – cardiac output; Hb – hemoglobin, RDW – red cell distribution width; WBC – white blood cell count; BNP - Brain Natriuretic Peptide; ALP - alkaline phosphatase; ALT – alanine aminotransferase; AST – aspartate aminotransferase; HDL - high density lipoprotein; LDL - low density lipoprotein; TG - triglycerides; FEV1 – forced expiratory volume; FVC – forced vital capacity; KCO – transfer coefficient for carbon monoxide.

	[ALL] N=380	Control N=120	PAH N=260	p-value	N
Age at diagnosis	45 [34;59]		45 [34;59]		260
Age at sampling	52 [41;62]	51 [37;57]	53 [42;64]	0.019*	380
Diagnosis:					260
HPAH	27 (10%)		27 (10%)		
IPAH	233 (90%)		233 (90%)		
Case:					260
incident	51 (20%)		51 (20%)		
prevalent	209 (80%)		209 (80%)		
Gender: female	267 (70%)	77 (64%)	190 (73%)	0.100	380
BMI [kg/m²]	28 [24;32]	25 [24;30]	28 [24;32]	0.036	327
Ethnicity:				<0.001*	379
White	293 (77%)	66 (55%)	227 (88%)		
Asian	41 (11%)	22 (18%)	19 (7%)		
Black	10 (3%)	6 (5%)	4 (2%)		
Caribbean	1 (0%)	0 (0%)	1 (0%)		
Other	30 (8%)	24 (20%)	6 (2%)		
Not stated	4 (1%)	2 (2%)	2 (1%)		
Smoking history:				<0.001*	354
no	205 (58%)	88 (86%)	117 (46%)		
past/current	149 (42%)	14 (14%)	135 (54%)		
Systemic hypertension	74 (20%)	20 (20%)	54 (21%)	0.919	362
Coronary artery disease	15 (4%)	7 (7%)	8 (3%)	0.140	362
Diabetes mellitus type 2	42 (12%)	3 (3%)	39 (15%)	0.002*	362
Dyslipidemia	31 (9%)	9 (9%)	22 (8%)	1.000	362
Hypothyroidism	42 (12%)	4 (4%)	38 (15%)	0.007*	362
Obstructive sleep apnoea	12 (3%)	0 (0%)	12 (5%)	0.023*	362

eTable 5. Clinical characteristics of patients and controls in whom BMP9 and pBMP10 measurements were undertaken. Data presented as: count (%), median [IQR], BMI – body mass index; there was no diagnosis of Hereditary Hemorrhagic Telangiectasia in the entire cohort. *significant after multiple testing correction by Benjamini & Hochberg (11).

AJRCCM Articles in Press. Published on 29-October-2019 as 10.1164/rccm.201906-1141OC

	Distribution across quartiles for combined control and PAH BMP9 values			
	0-25	**25-50**	**50-75**	**75-100**
BMP9 Males	C= 7/43 (16%) P= 21/70 (30%)	C= 14/43 (33%) P= 15/70 (21%)	C= 10/43 (23%) P= 18/70 (26%)	C= 12/43 (28%) P= 16/70 (23%)
BMP9 Females	C= 11/77 (14%) P= 56/190 (29%)	C= 26/77 (34%) P= 39/190 (21%)	C= 19/77 (23%) P= 46/190 (24%)	C= 21/77 (28%) P= 49/190 (26%)
	Distribution across quartiles for combined control and PAH pBMP10 values			
	0-25	**25-50**	**50-75**	**75-100**
pBMP10 Males	C= 7/43 (16%) P= 20/67 (30%)	C= 12/43 (28%) P= 15/70 (22%)	C= 12/43 (28%) P= 16/70 (24%)	C= 11/43 (26%) P= 16/70 (24%)
pBMP10 Females	C= 10/77 (13%) P= 56/187 (30%)	C= 20/77 (26%) P= 46/187 (25%)	C= 24/77 (31%) P= 42/187 (22%)	C= 23/77 (30%) P= 43/187 (23%)

eTable 6. PAH patients are overrepresented in the lowest 25% of plasma BMP9 and pBMP10 measurements for males and females. For BMP9, the values for controls (C) and PAH patients (P) were pooled for males and analysed. The median and 25% and 75% boundaries were determined for all the data values. The number of controls and PAH patients in each quartile were counted. The number of male controls in each quartile was expressed as a percentage of the total number of male control samples. Accordingly, the number of male PAH patients was expressed as the percentage of the total number of male PAH samples. The same approach was then applied to BMP9 levels in females and pBMP10 levels in males and in females. In all cases, the proportion of PAH patients falling in the 0-25% cluster was approximately double the percentage of controls falling in this quartile.

The proportion of individuals having both BMP9 and pBMP10 levels in their lowest quartile were 1/7 (14%) control males and 8/77 (10%) control females. In contrast, a higher proportion of PAH patients with both BMP9 and pBMP10 levels in the lowest quartile were represented for males (14/21 (67%) for BMP9 and 14/20 (70%) for pBMP10) and females (38/56 (68%) for BMP9 and pBMP10).

	[ALL] N=260	Lower tertile N=94	Middle tertile N=80	Higher tertile N=86	p-overall*	N
Demographics and functional status						
Age at sampling	53 [42;64]	54 [42;67]	49 [41;63]	56 [44;64]	0.261	260
Gender: female	190 (73%)	57 (61%)	60 (75%)	73 (85%)	**0.001**	260
BMI [kg/m²]	27 [24;32]	28 [25;32]	27 [24;31]	27 [22;31]	0.263	174
WHO class:					0.178	258
1	31 (12%)	6 (6%)	13 (16%)	12 (14%)		
2	99 (38%)	39 (41%)	29 (37%)	31 (36%)		
3	115 (45%)	46 (49%)	30 (38%)	39 (46%)		
4	13 (5%)	3 (3%)	7 (9%)	3 (4%)		
6MWD [m]	389 [335;452]	394 [366;428]	370 [288;481]	390 [336;435]	0.772	116
Shuttle walk test [m]	375 [304;515]	418 [312;625]	330 [275;431]	388 [341;460]	0.558	30
Hemodynamics						
mRAP [mmHg]	10 [4;12]	9 [5;13]	8 [4;12]	11 [8;12]	0.326	38
mPAP [mmHg]	49 [39;63]	47 [32;50]	42 [36;58]	59 [42;66]	0.158	39
PVR [WU]	8.05 [5.72;13.9]	8.05 [6.45;12.8]	7.40 [4.00;10.9]	10.4 [6.20;17.4]	0.430	36
CO [L/min]	4.7 (2.1)	4.6 (2.3)	5.3 (2.0)	4.1 (2.0)	0.289	38
Lung function						
FEV1 [% pred.]	86 (20)	87 (21)	83 (19)	88 (19)	0.763	58
FVC [% pred.]	99 (21)	97 (21)	99 (23)	99 (20)	0.950	59
KCO [% pred.]	77 (16)	81 (14)	67 (17)	82 (11)	**0.016**	36
Clinical blood tests						
Hb [g/l]	141 [130;152]	146 [128;157]	141 [133;152]	139 [128;148]	0.148	239
RDW [%]	14 [14;16]	15 [14;16]	14 [14;16]	14 [14;15]	**0.007**	173
WBC [x10e9/l]	7.0 [5.5;8.6]	7.3 [6.0;9.1]	7.0 [5.3;8.3]	6.5 [5.3;8.4]	0.083	240
Plt [x10e9/l]	212 [170;259]	188 [158;238]	221 [179;264]	224 [175;271]	**0.016**	240
Albumin [g/l]	42 [39;45]	42 [38;44]	43 [40;46]	42 [39;45]	0.072	249
ALP [IU/l]	79 [62,101]	84 [62;118]	76 [61;88]	81 [63;99]	0.222	247
ALT [IU/l]	21 [16;27]	20 [15;28]	22 [16;29]	21 [16;26]	0.532	248
AST [IU/l]	24 [19;28]	22 [18;28]	23 [19;28]	24 [20;28]	0.585	181
Bilirubin [µmol/l]	10 [8;14]	11 [8;16]	9 [8;14]	9 [7;13]	0.069	249
CRP [mg/l]	2 [1;6]	5 [2;11]	2 [1;5]	2 [1;3]	**0.001**	174
Total protein [g/l]	72 [68;75]	71 [66;76]	72 [68;74]	71 [69;74]	0.925	189
Sodium [mmol/l]	140 [139;141]	140 [138;141]	140 [139;142]	140 [139;142]	0.841	244
Potassium [mmol/l]	4.1 (0.4)	4.2 (0.5)	4.1 (0.4)	4.1 (0.4)	0.198	244
Urea [mmol/l]	5.6 [4.2;6.9]	5.9 [4.5;7.5]	5.5 [4.2;6.5]	5.6 [4.1;6.7]	0.123	244
Creatinine [mmol/l]	79 [68;97]	82 [69;102]	81 [68;98]	76 [66;91]	0.111	242
NTproBNP [ng/l]	222 [61.5;1230]	538 [81.0;1836]	151 [53.3;382]	176 [57.5;1126]	**0.031**	110
BNP [ng/l]	64.8 [30.1;167]	72.4 [29.0;147]	51.6 [28.5;200]	82.0 [36.7;146]	0.993	101
Comorbidities						
HTN	54 (21%)	24 (26%)	18 (22%)	12 (14%)	0.144	260
DM type 1	5 (2%)	2 (2%)	1 (1%)	2 (2%)	1.000	260
DM type 2	39 (15%)	14 (15%)	15 (19%)	10 (12%)	0.438	260
CAD	8 (3%)	3 (3%)	3 (4%)	2 (2%)	0.907	260
CVA	4 (2%)	3 (3%)	1 (1%)	0 (0%)	0.269	260
Dyslipidemia	22 (8%)	5 (5%)	12 (15%)	5 (6%)	**0.041**	260
AVM	2 (1%)	1 (1%)	1 (1%)	0 (0%)	0.760	260
Epistaxis	3 (1%)	1 (1%)	1 (1%)	1 (1%)	1.000	260
Hepatitis	4 (2%)	2 (2%)	1 (1%)	1 (1%)	1.000	260
Hypothyroidism	38 (15%)	16 (17%)	11 (14%)	11 (13%)	0.700	260
COPD	10 (4%)	6 (6%)	1 (1%)	3 (3%)	0.258	260
Asthma	28 (11%)	9 (10%)	9 (11%)	10 (12%)	0.894	260
OSA	12 (5%)	7 (7%)	4 (5%)	1 (1%)	0.112	260
Heterotaxia	1 (0%)	1 (1%)	0 (0%)	0 (0%)	1.000	260
Asplenia	1 (0%)	1 (1%)	0 (0%)	0 (0%)	1.000	260
Cancer	17 (7%)	6 (6%)	6 (8%)	5 (6%)	0.905	260

eTable 7. Clinical characteristics at the time of sampling of I/HPAH cases by BMP9 concentration tertiles. Tertiles' ranges: lower 0 – 186.7 pg/ml, middle 189.6 – 266.7 pg/ml, 267.1 – 591.2 pg/ml. Data presented as: † median [interquartile range], ^count (%), ‡ mean (SD), IPAH – idiopathic pulmonary arterial hypertension; HPAH – hereditary pulmonary arterial hypertension (diagnosis based on positive family history); BMI – body mass index; WHO class – World Health Organization functional class; 6MWT – 6 minute walk

AJRCCM Articles in Press. Published on 29-October-2019 as 10.1164/rccm.201906-1141OC

test; mRAP – mean right atrial pressure; mPAP – mean pulmonary arterial pressure; PVR –pulmonary vascular resistance; CO – cardiac output; FEV1 – forced expiratory volume; FVC – forced vital capacity; KCO – transfer coefficient for carbon monoxide; NO challenge – nitric oxide challenge; Hb – hemoglobin, RDW – red cell distribution width; WBC – white blood cell count; Plt – platelets; ALP – alkaline phosphatase; ALT – alanine aminotransferase; AST – aspartate aminotransferase; AVM - arteriovenous malformation (one hepatic AVM and one pulmonary AVM); CRP – C-reactive protein; DM type 1 - Diabetes mellitus type 1; DM type 2 - diabetes mellitus type 2; OSA - obstructive sleep apnoea; CAD - coronary artery disease; CVA - cardiovascular accident; HTN – systemic hypertension. *None of the comparisons remained significant after adjustment for multiple comparisons by Benjamini & Hochberg (11).

	[ALL] N=254	Lower tertile N=99	Middle tertile N=76	Higher tertile N=79	p-overall*	N
Demographics and functional status						
Age at sampling	53 [42;64]	55 [43;67]	52 [40;63]	51 [42;61]	0.243	254
Gender: female	187 (74%)	66 (67%)	56 (74%)	65 (82%)	0.063	254
BMI [kg/m²]	27 [24;32]	30 [26;33]	27 [24;31]	26 [21;29]	**0.004**	170
WHO class:					**0.005**	252
1	31 (12%)	3 (3%)	13 (17%)	15 (19%)		
2	96 (38%)	38 (39%)	29 (38%)	29 (37%)		
3	112 (44%)	53 (54%)	28 (37%)	31 (40%)		
4	13 (5%)	4 (4%)	6 (8%)	3 (4%)		
6MWD [m]	390 [335;460]	385 [308;420]	380 [315;481]	415 [370;462]	0.305	113
Shuttle walk test [m]	370 [300;500]	340 [300;520]	380 [320;500]	370 [332;436]	0.867	29
Hemodynamics						
mRAP[mmHg]	10 [4;12]	9 [7;13]	12 [4;12]	9 [5;11]	0.900	38
mPAP[mmHg]	49 [39;63]	40 [38;49]	48 [36;60]	60 [44;65]	0.186	39
PVR [WU]	8.05 [5.72;13.9]	6.10 [3.25;10.7]	7.70 [5.78;10.1]	11.8 [6.80;17.4]	0.138	36
CO[L/min]	4.7 (2.1)	4.5 (2.3)	5.4 (2.2)	4.1 (1.8)	0.315	38
Lung function						
FEV1[% pred.]	86 (20)	83 (18)	88 (21)	86 (21)	0.720	56
FVC[% pred.]	99 (21)	92 (19)	105 (23)	99 (21)	0.194	57
KCO[% pred.]	76 (15)	74 (19)	71 (16)	81 (11)	0.233	35
Clinical blood tests						
Hb [g/l]	140 [129;152]	140 [122;154]	141 [132;152]	140 [130;150]	0.802	233
RDW [%]	14 [14;15]	15 [14;16]	14 [14;16]	14 [13;15]	**0.004**	168
WBC [x10e9/l]	7.0 [5.5;8.6]	7.4 [5.8;9.0]	7.0 [5.8;8.3]	6.5 [5.1;8.1]	**0.041**	234
Plt [x10e9/l]	212 [170;260]	196 [161;262]	231 [175;270]	203 [170;246]	0.151	234
Albumin [g/l]	42 [39;45]	41 [37;45]	42 [40;46]	43 [40;46]	**0.017**	243
ALP [IU/l]	79 [62;101]	85 [66;111]	69 [57;88]	82 [62;100]	0.004	241
ALT [IU/l]	21 [16;27]	21 [16;29]	20 [15;24]	22 [17;28]	0.191	242
AST [IU/l]	23 [19;28]	23 [19;28]	22 [19;26]	24 [20;31]	0.158	177
Bilirubin [µmol/l]	10 [8;14]	10 [8;14]	9 [8;14]	10 [7;14]	0.750	243
CRP [mg/l]	2 [1;6]	4 [2;10]	2 [1;4]	2 [1;3]	**0.001**	171
Total protein [g/l]	72 [68;75]	72 [67;75]	72 [68;75]	71 [68;74]	0.729	185
Sodium [mmol/l]	140 [139;141]	140 [138;141]	140 [139;142]	140 [139;142]	0.251	238
Potassium [mmol/l]	4.1 (0.4)	4.2 (0.5)	4.1 (0.4)	4.1 (0.4)	0.373	238
Urea [mmol/l]	5.6 [4.2;7.0]	5.8 [4.2;7.5]	5.6 [4.5;6.5]	5.2 [4.0;6.5]	0.179	238
Creatinine [mmol/l]	80 [68;96]	82 [69;100]	79 [68;96]	77 [67;91]	0.181	236
NTproBNP [ng/l]	223 [61.5;1230]	332 [75.7;1849]	167 [59.0;984]	191 [60.0;839]	0.242	106
BNP [ng/l]	61.7 [30.1;148]	59.2 [28.8;143]	93.2 [39.9;156]	58.8 [30.5;169]	0.808	99
Comorbidities						
HTN	53 (21%)	29 (29%)	16 (21%)	8 (10%)	**0.008**	254
DM type 1	5 (2%)	2 (2%)	1 (1%)	2 (3%)	1.000	254
DM type 2	38 (15%)	22 (22%)	11 (14%)	5 (6%)	**0.013**	254
CAD	7 (3%)	3 (3%)	4 (5%)	0 (0%)	0.106	254
CVA	4 (2%)	2 (2%)	2 (3%)	0 (0%)	0.471	254
Dyslipidemia	21 (8%)	5 (5%)	9 (12%)	7 (9%)	0.263	254
AVM	2 (1%)	1 (1%)	1 (1%)	0 (0%)	0.757	254
Epistaxis	3 (1%)	1 (1%)	1 (1%)	1 (1%)	1.000	254
Hepatitis	4 (2%)	3 (3%)	1 (1%)	0 (0%)	0.317	254
Hypothyroidism	37 (15%)	16 (16%)	12 (16%)	9 (11%)	0.627	254
COPD	8 (3%)	5 (5%)	3 (4%)	0 (0%)	0.101	254
Asthma	27 (11%)	10 (10%)	7 (9%)	10 (13%)	0.766	254
OSA	11 (4%)	8 (8%)	2 (3%)	1 (1%)	0.086	254
Heterotaxia	1 (0%)	1 (1%)	0 (0%)	0 (0%)	1.000	254
Asplenia	1 (0%)	1 (1%)	0 (0%)	0 (0%)	1.000	254
Cancer	16 (6%)	7 (7%)	5 (7%)	4 (5%)	0.899	254

eTable 8. Clinical characteristics at the time of sampling of I/HPAH cases by pBMP10 concentration tertiles. Tertiles' ranges: lower 0 – 5105 pg/ml, middle 5151 – 7699 pg/ml, 7702 – 17806 pg/ml. Data presented as: † median [interquartile range], ^count (%), ‡ mean (SD), IPAH – idiopathic pulmonary arterial hypertension; HPAH – hereditary pulmonary arterial hypertension (diagnosis based on positive family history); BMI – body mass index; WHO FC class – World Health Organization functional class; 6MWD – 6 minute walk

AJRCCM Articles in Press. Published on 29-October-2019 as 10.1164/rccm.201906-1141OC

distance; mRAP – mean right atrial pressure; mPAP – mean pulmonary arterial pressure; PVR – pulmonary vascular resistance; CO – cardiac output; FEV1 – forced expiratory volume; FVC – forced vital capacity; KCO – transfer coefficient for carbon monoxide; NO challenge – nitric oxide challenge; Hb – hemoglobin, RDW – red cell distribution width; WBC – white blood cell count; Plt – platelets; ALP – alkaline phosphatase; AST – aspartate aminotransferase; ALT – alanine aminotransferase; AVM - arteriovenous malformation (one hepatic AVM and one pulmonary AVM); DM type 1 - Diabetes mellitus type 1; DM type 2 - diabetes mellitus type 2; OSA - obstructive sleep apnoea; CAD - coronary artery disease; CVA - cardiovascular accident; HTN - systemic hypertension; *None of the comparisons remained significant after adjustment for multiple comparisons by Benjamini & Hochberg (11).

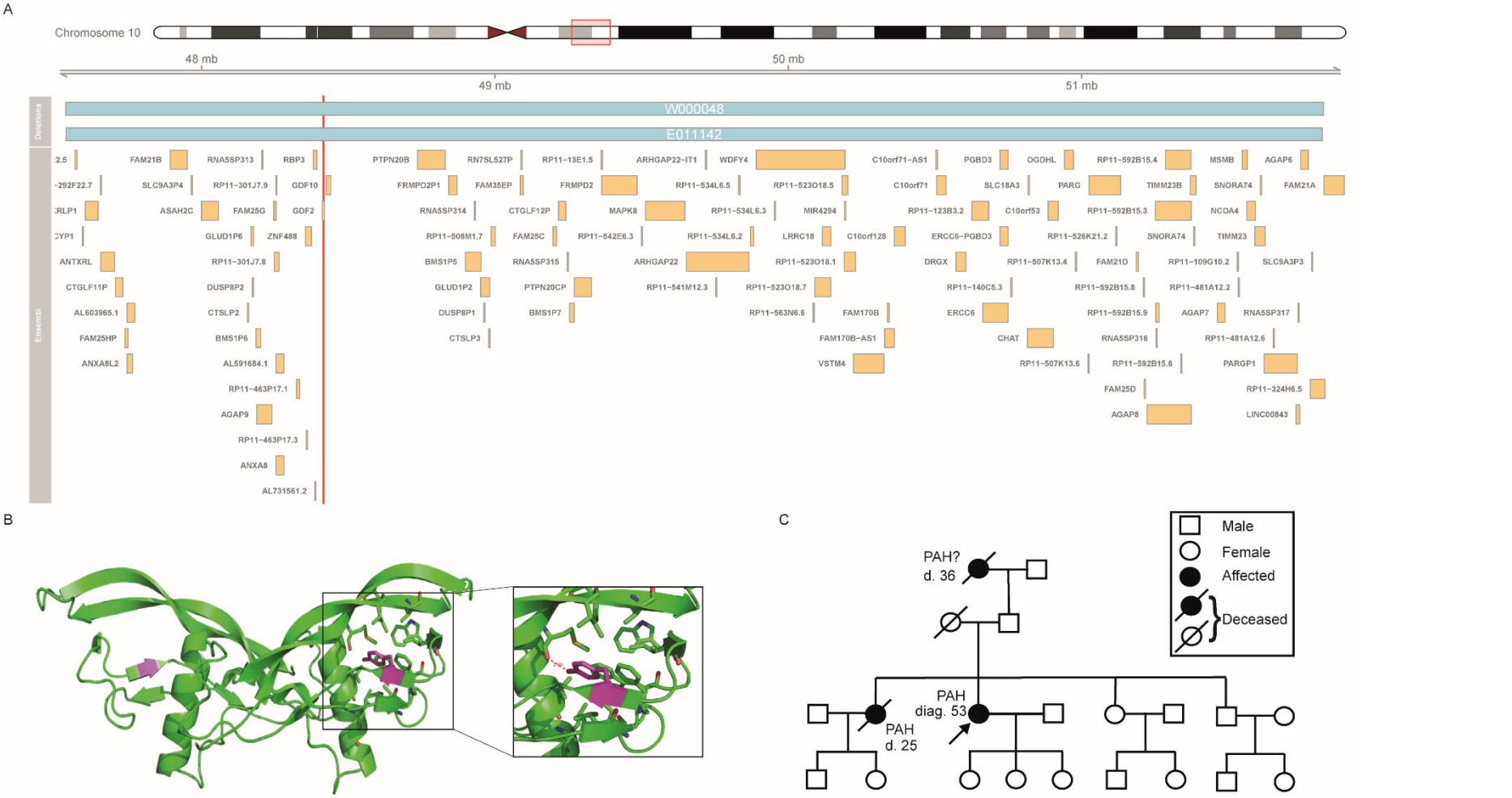

eFigure 1: Mutations in BMP9 (a) Large scale deletions leading to loss of the GDF2 allele and surrounding genes in two patients with PAH. The region of Chromosome 10 that is deleted is indicated by a box. The turquoise boxes show the coverage of the two deletions and the red vertical line indicates the position of the *GDF2* gene, encoding BMP9. (b) Mapping of the position of Tyrosine-351 on the BMP9 structure (Magenta). This Tyrosine forms a hydrogen bond with Methionine-421, an interaction which will be disrupted by the amino acid substitution in the Y351H mutant and may lead to destabilisation of the GFD due to disruption of the hydrophobic core. (c) Familial clustering of the PAH phenotype with the Adenine-to-Guanosine Mutation at Position 265 of the *GDF2* gene leading to the M89V Missense Mutation in BMP9. The arrow indicates the proband. Whole genome sequencing data was only available for the proband.

AJRCCM Articles in Press. Published on 29-October-2019 as 10.1164/rccm.201906-1141OC

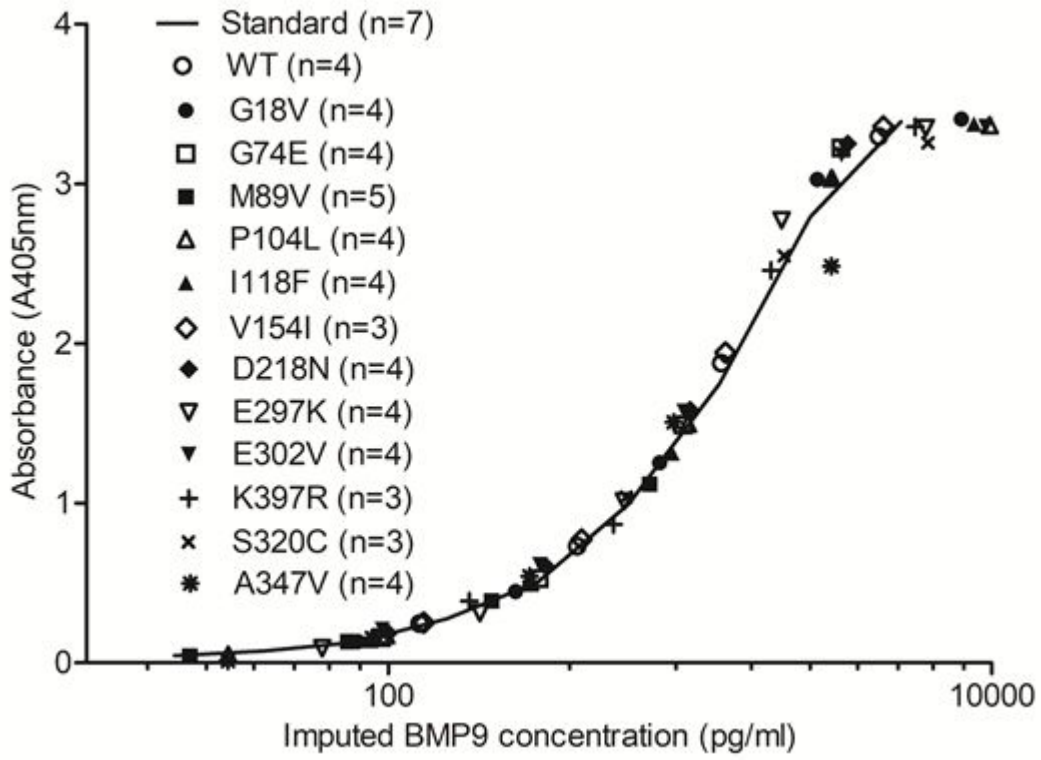

eFigure 2: Efficiency curves for the ELISA analysis of each BMP9 mutant variant. Concentration curves of the BMP9 mutants were analysed by ELISA and the BMP9 GFD concentrations determined. Plotting of the calculated BMP9 GFD dilutions against the absorbances confirmed that the BMP9 mutant curves superimposed on the BMP9-WT curve, indicating that the efficiencies of binding in the ELISA were equivalent. n = number of points fitted for each sample.

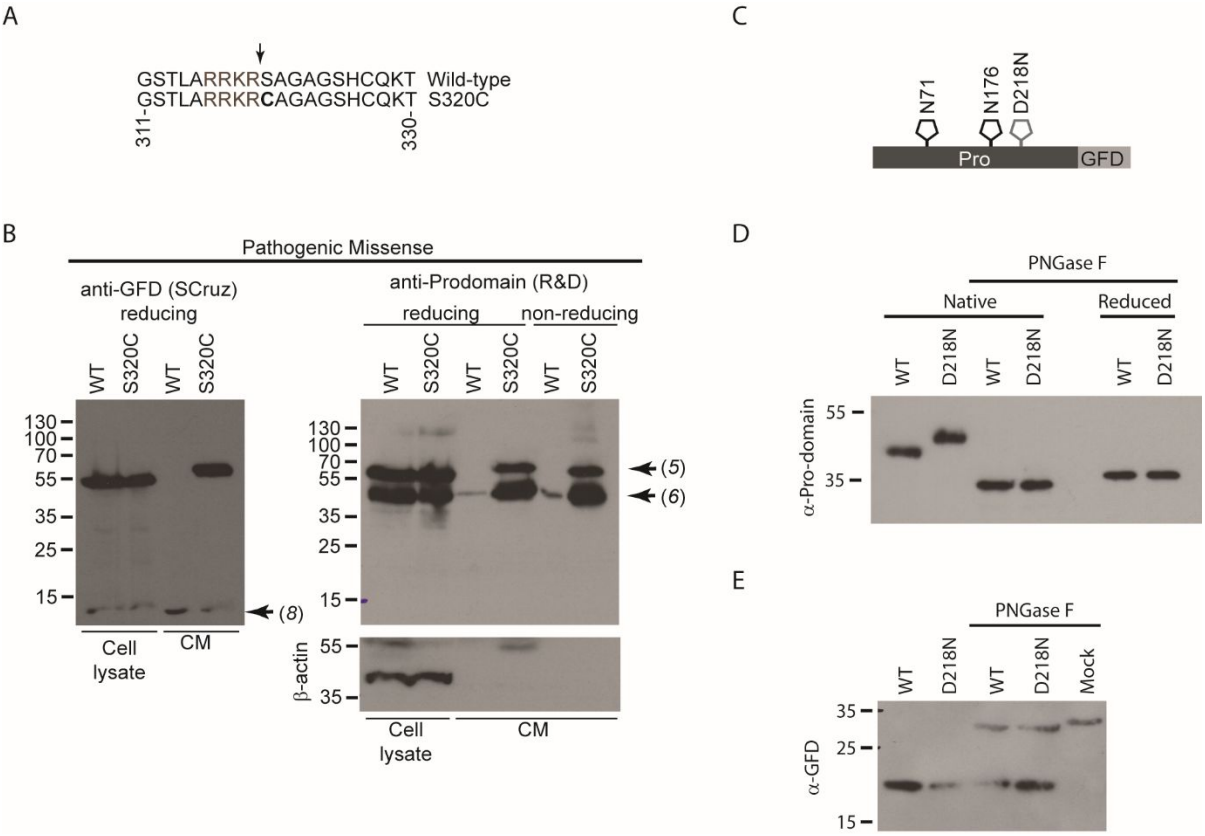

eFigure 3: Altered glycosylation of the BMP9-D218N variant and impaired furin processing of the BMP9-S320C mutant. (a) Comparison of the partial protein sequences indicating the position of the S320C missense mutation (Substituted C in bold) adjacent to the consensus RRKR furin cleavage motif in the *ProBMP9* precursor. (b) Western blotting of cell lysates and conditioned media from HEK-EBNA cells exogenously expressing BMP9-wt and BMP9-S320C were analysed by Western blotting. The GFD was analysed by reducing SDS-PAGE (right panel) and prodomain analysed by under both reducing conditions (in cells and conditioned media) and non-reducing conditions (conditioned media). The numbered arrows indicate the nature of the processed forms as defined in Figure 1a. (c) In silico prediction of the glycosylation of the BMP9-D218N variant, showing the two consensus glycosylation sites (Black) at Arginine-71 (N71) and Arginine-176 (N176) and the predicted *de novo* site introduced by the change from Aspartic acid to Arginine at position 218. (b-c) The media from HEK-EBNA cells exogenously expressing BMP9-WT and BMP9-D218N were subject to deglycosylation followed by Western blotting for (d) the BMP9 prodomain or (e) BMP9 GFD. All blots are representative of n=3 experiments.

AJRCCM Articles in Press. Published on 29-October-2019 as 10.1164/rccm.201906-1141OC

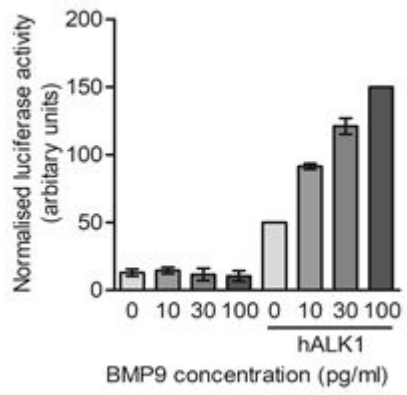

eFigure 4: Dose response of C2C12 myoblasts transfected with or without hALK1. C2C12 mouse myoblast cells were transfected with BRE-firefly reporter and thymidine kinase-Renilla normalisation plasmids. A hALK1 expression vector was added to the transfection mix for some wells. Serum starved cells were treated with BMP9-WT for 6 hours before luminescence was determined.

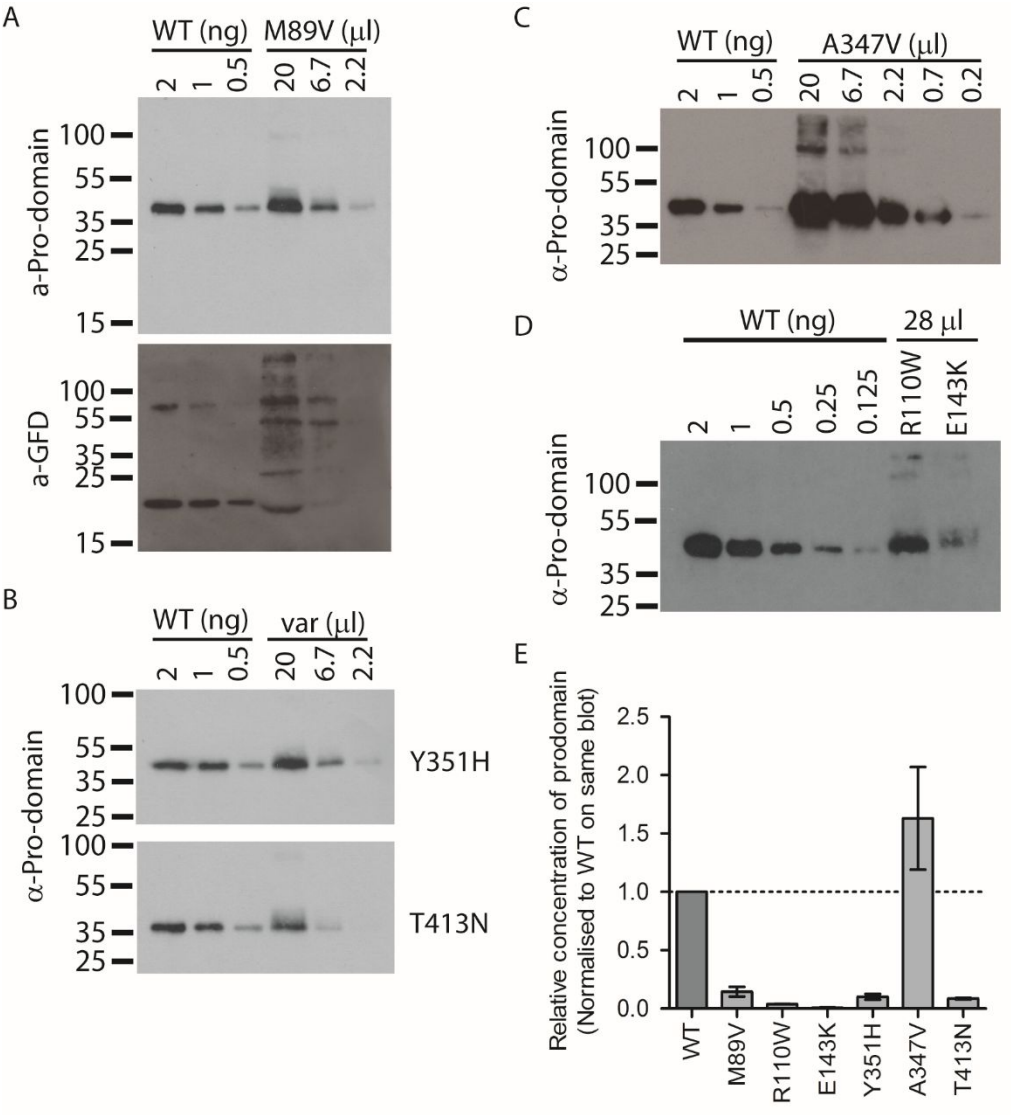

eFigure 5: Titration of BMP9 variants against BMP9-WT. Dilutions of conditioned media containing BMP9-WT (a-d) or the BMP9 variants: (a) M89V, (b) Y351H and T413N), (c) A347V and (d) R110W and E143K, were analysed by western blotting. (e) The relative amounts of each mutant were quantified by densitometry relative to the WT on the same blot to calculate relative expression values. Data are mean from n=3 blots for each variant.

AJRCCM Articles in Press. Published on 29-October-2019 as 10.1164/rccm.201906-1141OC

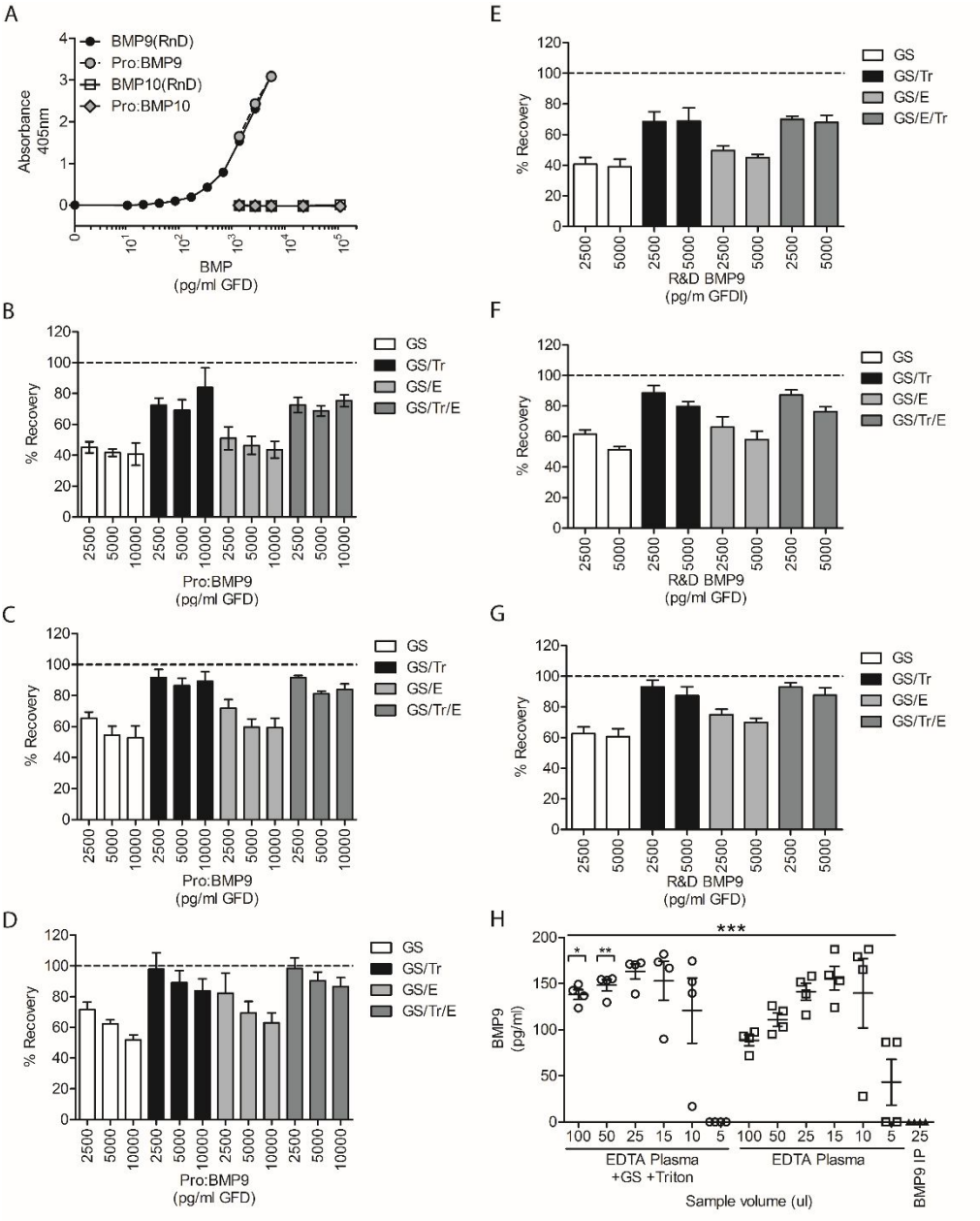

eFigure 6: Validation of BMP9 GFD ELISA protocol for human plasma. All concentrations of BMPs in panels a-d are presented as GFD equivalents. (a) Cross-reactivity assessment showing the BMP9 ELISA detects the BMP9-GFD and Pro:BMP9 with equivalence, whereas BMP10-GFD and Pro:BMP10 do not cross-react. Data are representative of 3 separate experiments. (b-d) The effect of Triton-X100 (0.5%) and EDTA (4.5mM) alone, or in combination, on the efficiency of Pro:BMP9 recovery (assay buffer supplemented to 0.2% goat serum (GS)) from plasma volumes of (b) 25µl, (c) 15µl and (d) 10µl. (e-g). The effect of Triton X-100 (0.5%) and EDTA (4.5mM) alone, or in combination, on the efficiency of Pro:BMP9 recovery (assay buffer supplemented to 0.2% goat serum (GS)) from plasma volumes of (e) 25µl, (f) 15µl and (g) 10µl. Data in b-g are mean of 3 separate experiments, each experiment using plasma from a different healthy male control. (h) Comparison of the measured levels of BMP9 in different volumes of plasma alone 5-100µl, or with supplementation with 0.5% Triton-X100 and 0.2% goat serum. Immunoprecipitation of BMP9 confirmed that the ELISA was specifically detecting BMP9 in plasma. Data are mean ± SEM, n=4. Two-way ANOVA; **P*<0.05, ***P*<0.01 ****P*<0.001

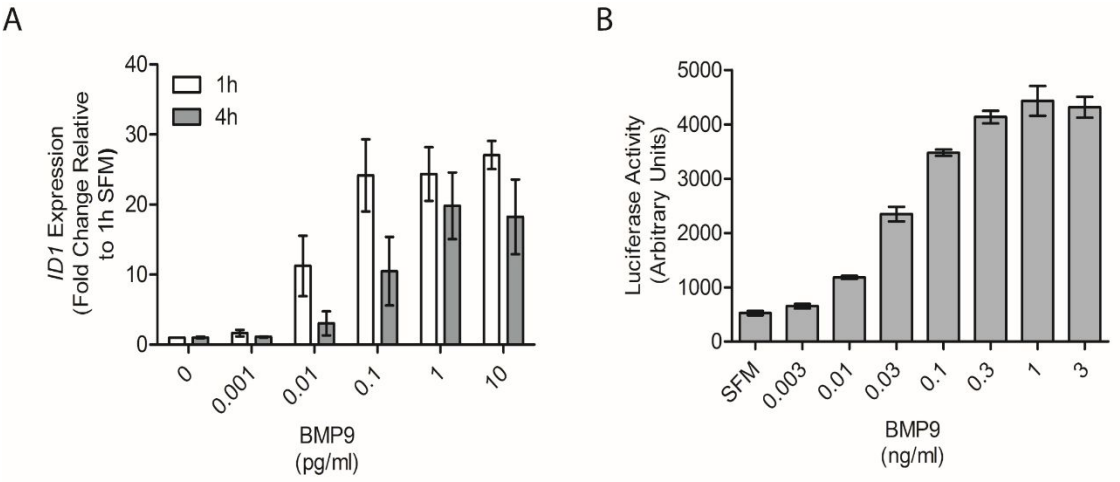

eFigure 7: Confirmation of high affinity BMP9 responses in the HMEC1-BRE luciferase stable reporter line. (a) Untransduced HMEC1 cells were treated with BMP9 (0.001-10ng/ml) in SFM for 1 hour or 4 hours and lysed for RNA. QPCR analysis of ID2 induction, normalized to B2M, was assessed. Data are mean ± SEM for n=3 experiments. (b) HMEC1-BRE cells were treated with BMP9 (0.003-3ng/ml) for 6 hours, followed by assay of luciferase activity. Data are representative of 3 separate experiments (n=4 wells/treatment).

AJRCCM Articles in Press. Published on 29-October-2019 as 10.1164/rccm.201906-1141OC

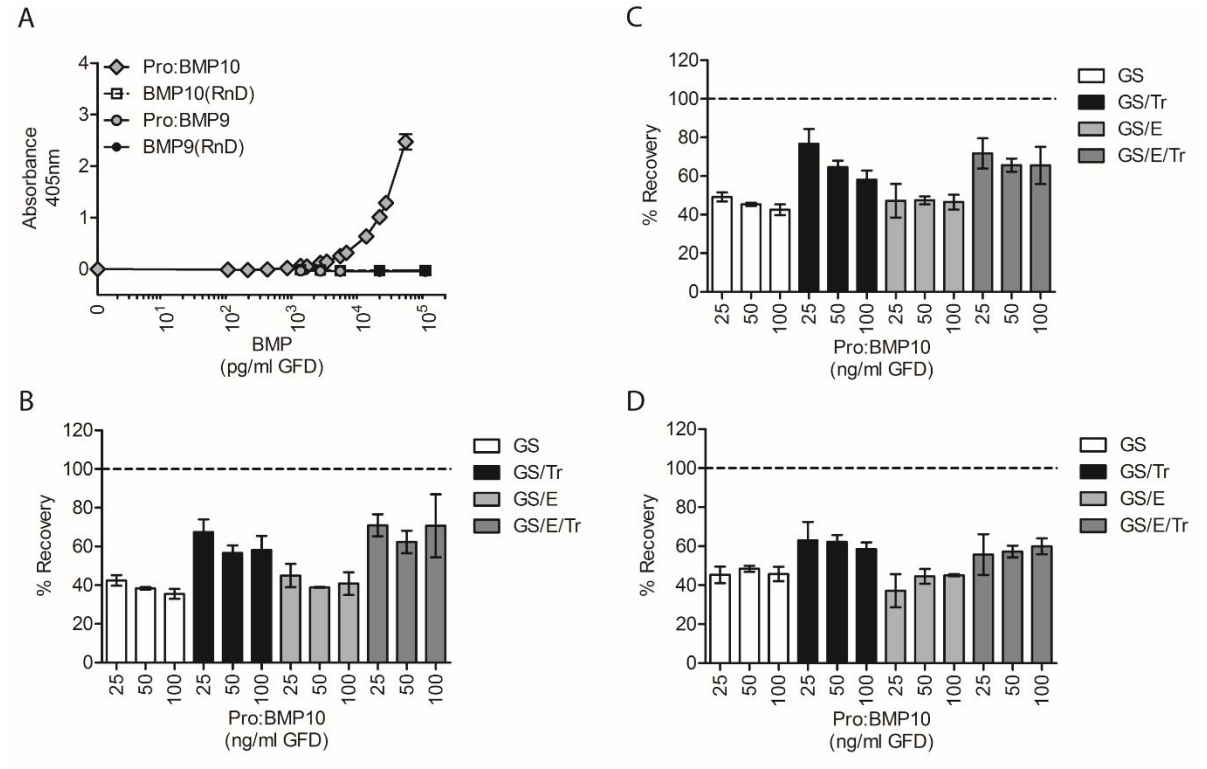

eFigure 8: Validation of pBMP10 ELISA protocol for human plasma. All concentrations of BMPs in panels a-d are presented as GFD equivalents. (a) Cross-reactivity assessment showing the pBMP10 ELISA detects Pro:BMP9, but not the BMP10 GFD, nor BMP9-GFD or Pro:BMP9. Data are representative of 3 separate experiments. (b-d) The effect of Triton-X100 (0.5%) and EDTA (4.5mM) alone, or in combination, on the efficiency of Pro:BMP10 recovery (assay buffer supplemented to 0.2% goat serum (GS)) from plasma volumes of (b) 25µl, (c) 15µl and (d) 10µl. Data in b-g are mean of 3 separate experiments, each experiment using plasma from a different healthy male control.

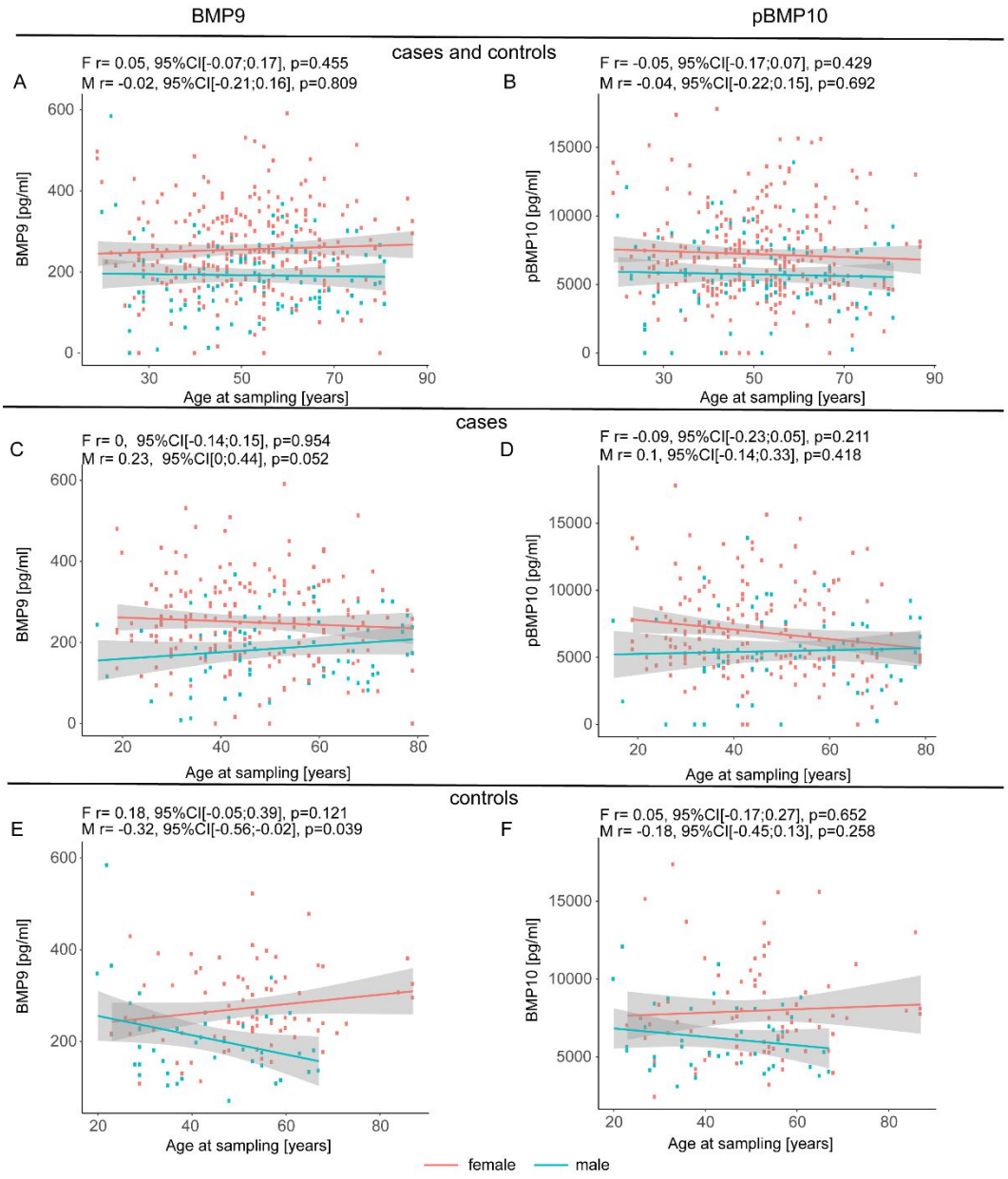

eFigure 9: BMP9 and pBMP10 levels do not correlate with age for males or females in cases and controls. The levels of BMP9 and pBMP10 were assessed regarding any correlation to age for males or females using a Spearman test for (a-b) combined cases and controls, (c-d) cases only or (e-f) controls only.

AJRCCM Articles in Press. Published on 29-October-2019 as 10.1164/rccm.201906-1141OC

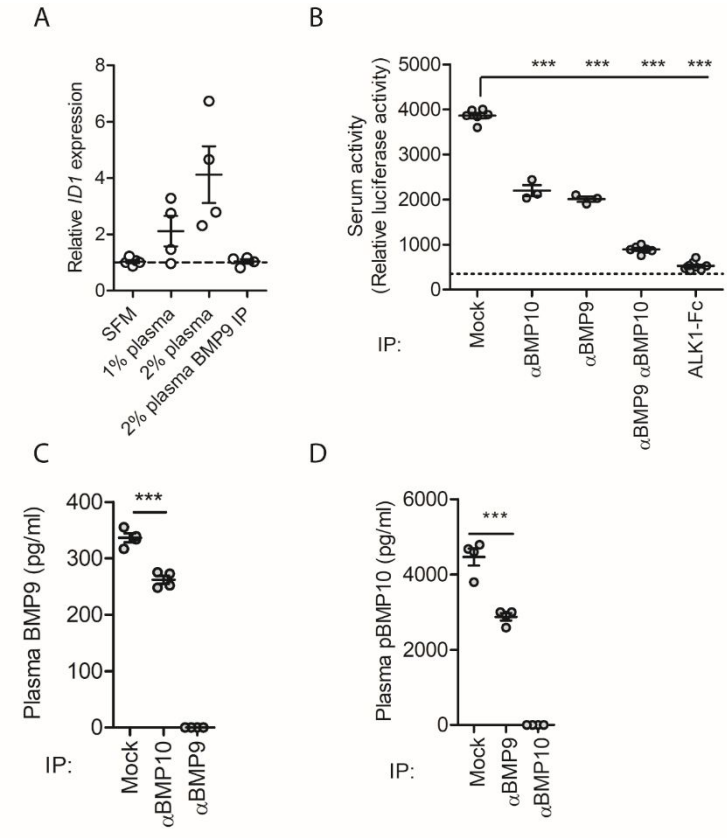

eFigure 10: Circulating BMP9 and pBMP10 are physically associated. (a) Endothelial cells were incubated with neat plasma from 4 different male donors or plasma from which BMP9 had been immunoprecipitated. After 8 hours, endothelial cell RNA was extracted and QPCR undertaken for *ID1* and calculated as expression relative to *B2M* using the ΔΔCT method. (b) HMEC1-BRE cells quiesced in serum free media overnight were treated with 10% serum from 4 different male donors, from which BMP9 or BMP10 had been immunoprecipitated with the indicated reagents, for 6 hours before luciferase activity was assessed. (c) BMP9 GFD and (d) pBMP10 concentration in EDTA-plasma immunoprecipitated with the indicated antibodies was assessed by ELISA Data are mean ± SEM; n=4, one-way ANOVA. Dotted lines represent basal activity of untreated cells.

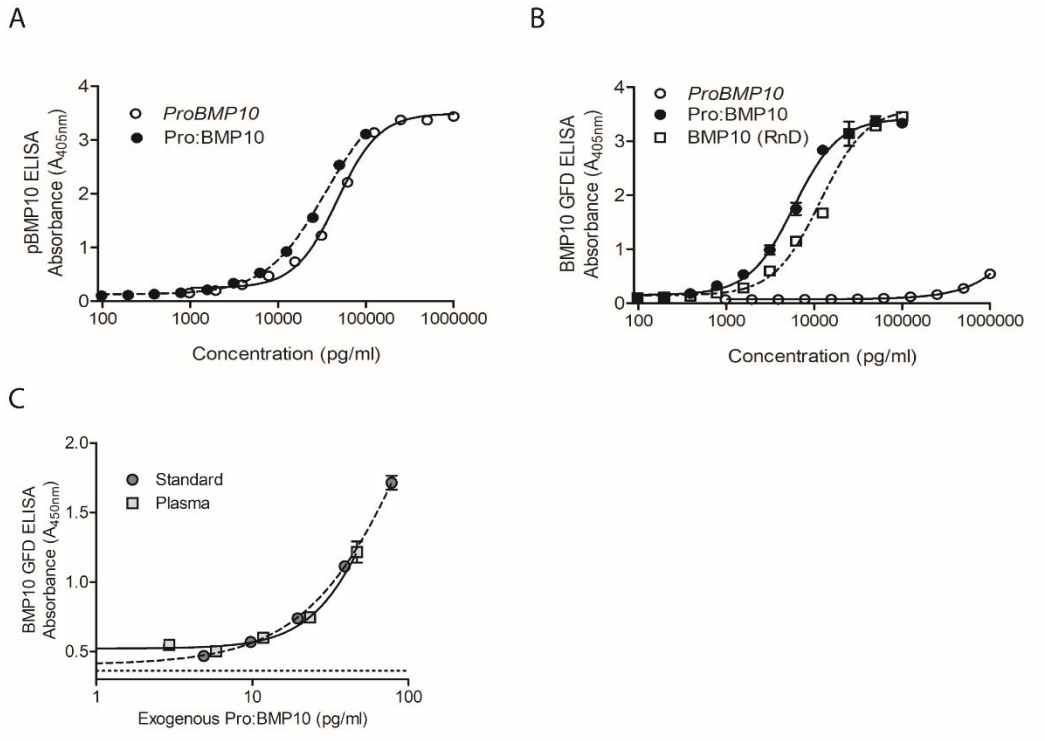

eFigure 11: The majority of plasma pBMP10 is unprocessed. All concentrations of BMPs in panels are presented as GFD equivalents. (a) Cross-reactivity assessment showing the pBMP10 ELISA detects Pro:BMP10 and *ProBMP10* (b) Cross-reactivity assessment showing the BMP10 GFD ELISA detects BMP10 GFD and Pro:BMP10 but not *ProBMP10* (c) Pro:BMP10 was spiked into EDTA-plasma, and recovery efficiency was assessed compared to Pro:BMP10 spiked into ELISA diluent. The dotted horizontal lines represent the blank measurement. Data are representative of 3 separate experiments.

AJRCCM Articles in Press. Published on 29-October-2019 as 10.1164/rccm.201906-1141OC

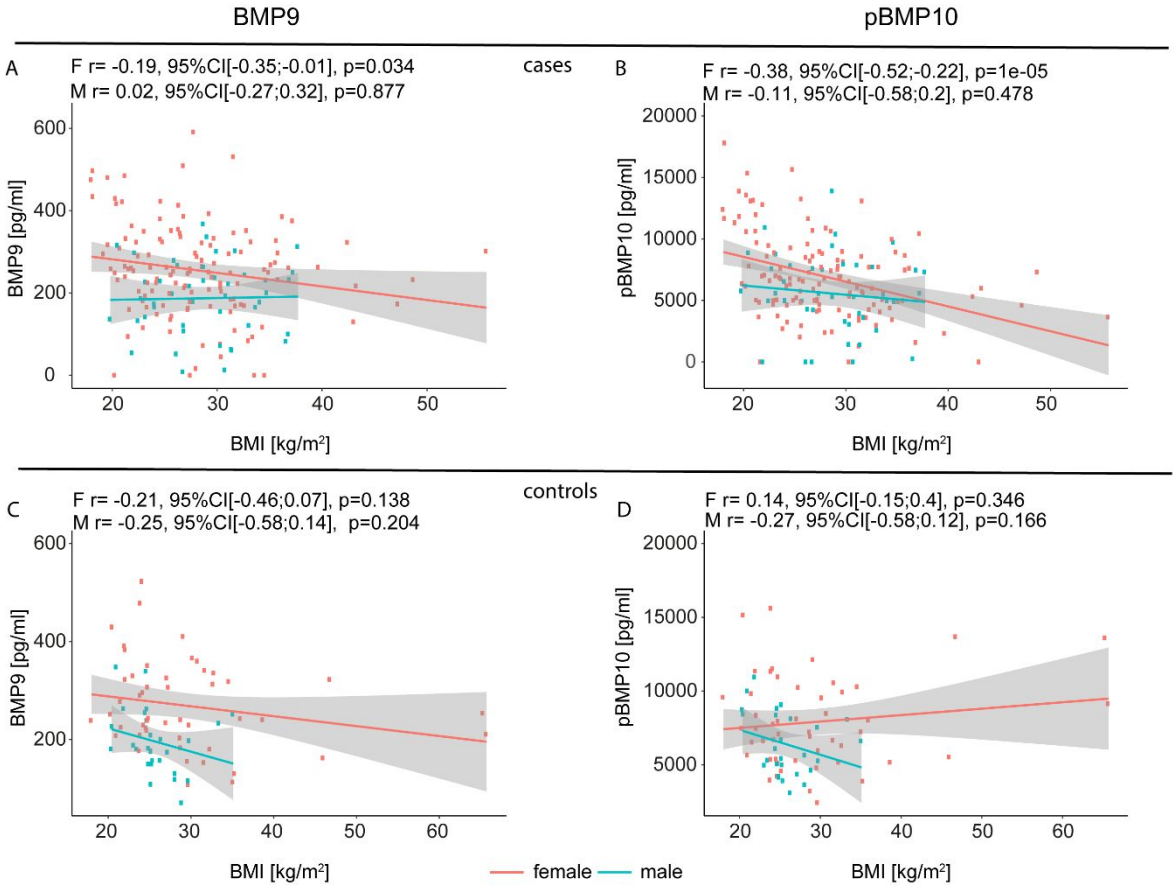

eFigure 12: BMP9 and pBMP10 levels negatively correlate with BMI in PAH cases, but not controls. The levels of BMP9 and pBMP10 were assessed regarding any correlation to BMI for males or females using a Spearman test for (a-b) cases or (c-d) controls.

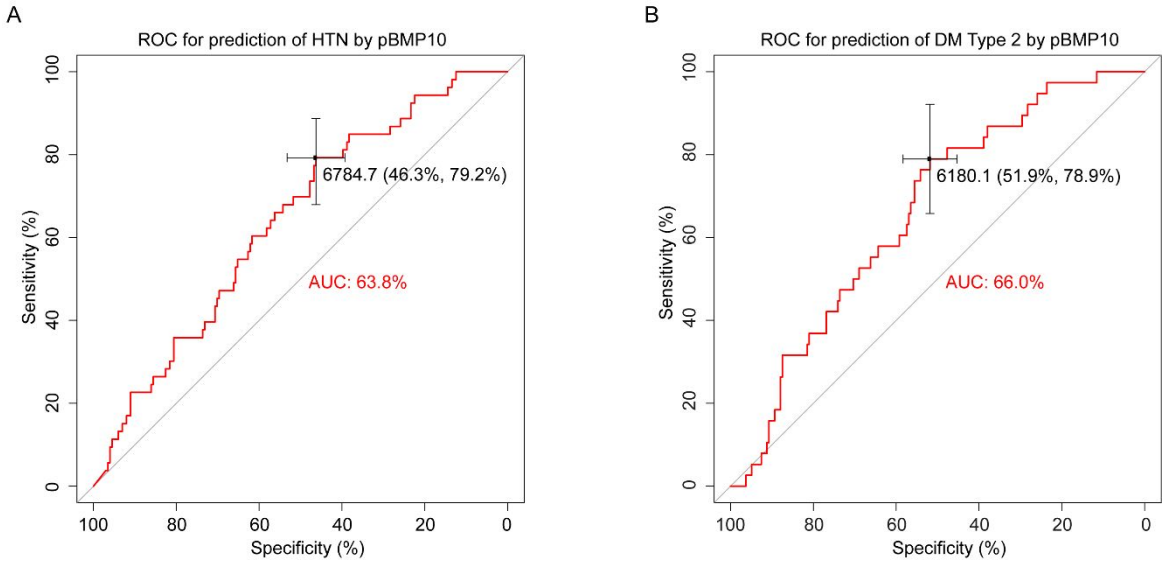

eFigure 13: ROC curves for pBMP10 measurements as a predictor of systemic hypertension (HTN) and diabetes mellitus type 2 in I/HPAH patients. ROC analysis for pBMP10 levels as a predictor of (a) systemic hypertension (HTN) and (b) diabetes mellitus type 2. The diagonal line indicates the line of no discrimination.

AJRCCM Articles in Press. Published on 29-October-2019 as 10.1164/rccm.201906-1141OC

A

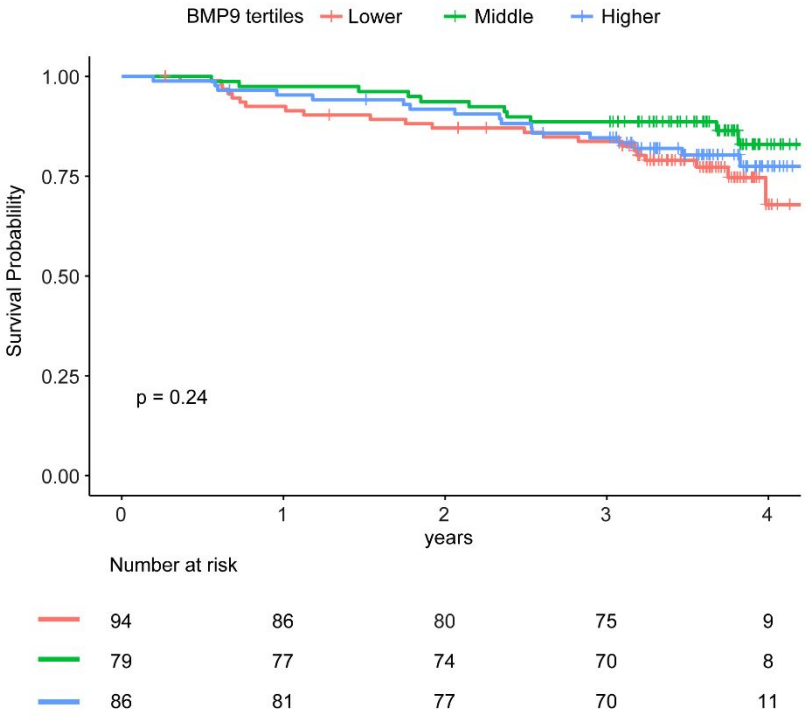

B

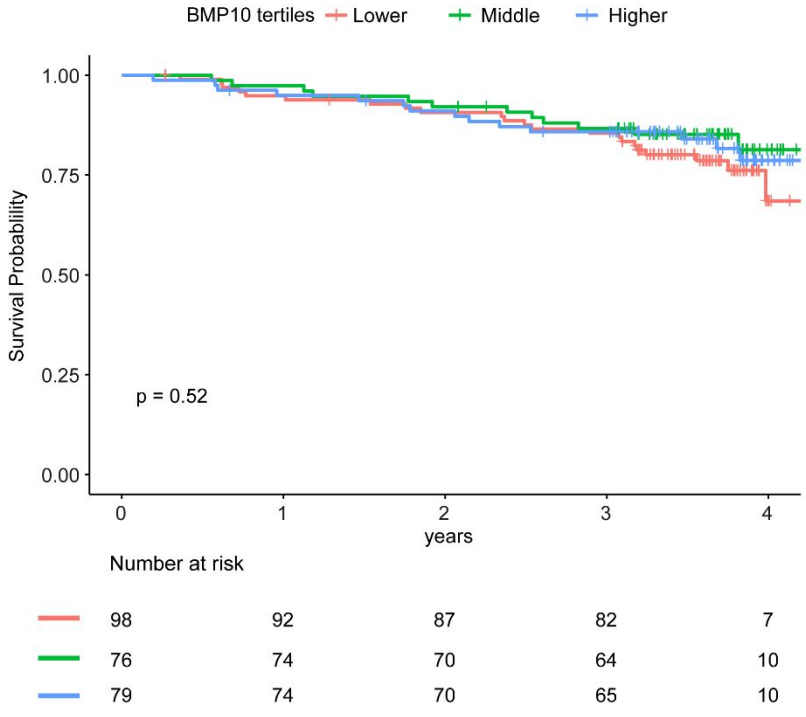

eFigure 14. Kaplan-Meier survival curves for BMP9 and pBMP10 tertiles.

References

1. Gräf S, Haimel M, Bleda M, Hadinnapola C, Southgate L, Li W, Hodgson J, Liu B, Salmon RM, Southwood M, Machado RD, Martin JM, Treacy CM, Yates K, Daugherty LC, Shamardina O, Whitehorn D, Holden S, Aldred M, Bogaard HJ, Church C, Coghlan G, Condliffe R, Corris PA, Danesino C, Eyries M, Gall H, Ghio S, Ghofrani H-A, Gibbs JSR, Girerd B, Houweling AC, Howard L, Humbert M, Kiely DG, Kovacs G, MacKenzie Ross RV, Moledina S, Montani D, Newnham M, Olschewski A, Olschewski H, Peacock AJ, Pepke-Zaba J, Prokopenko I, Rhodes CJ, Scelsi L, Seeger W, Soubrier F, Stein DF, Suntharalingam J, Swietlik EM, Toshner MR, van Heel DA, Vonk Noordegraaf A, Waisfisz Q, Wharton J, Wort SJ, Ouwehand WH, Soranzo N, Lawrie A, Upton PD, Wilkins MR, Trembath RC, Morrell NW. Identification of rare sequence variation underlying heritable pulmonary arterial hypertension. *Nat Commun* 2018;9:1416.
2. Kircher M, Witten DM, Jain P, O'Roak BJ, Cooper GM, Shendure J. A general framework for estimating the relative pathogenicity of human genetic variants. *Nature genetics* 2014;46:310-315.
3. Adzhubei IA, Schmidt S, Peshkin L, Ramensky VE, Gerasimova A, Bork P, Kondrashov AS, Sunyaev SR. A method and server for predicting damaging missense mutations. *Nat Methods* 2010;7:248-249.
4. Ng PC, Henikoff S. Predicting deleterious amino acid substitutions. *Genome Res* 2001;11:863-874.
5. Cooper GM, Stone EA, Asimenos G, Green ED, Batzoglou S, Sidow A, Progra NCS. Distribution and intensity of constraint in mammalian genomic sequence. *Genome Res* 2005;15:901-913.
6. Ormiston ML, Toshner MR, Kiskin FN, Huang CJZ, Groves E, Morrell NW, Rana AA. Generation and culture of blood outgrowth endothelial cells from human peripheral blood. *Jove-J Vis Exp* 2015;106:e53384.
7. Korchynskyi O, ten Dijke P. Identification and functional characterization of distinct critically important bone morphogenetic protein-specific response elements in the id1 promoter. *JBiolChem* 2002;277:4883-4891.
8. Jiang H, Salmon RM, Upton PD, Wei Z, Lawera A, Davenport AP, Morrell NW, Li W. The prodomain-bound form of bone morphogenetic protein 10 is biologically active on endothelial cells. *J Biol Chem* 2016;291:2954-2966.
9. Wei Z, Salmon RM, Upton PD, Morrell NW, Li W. Regulation of bone morphogenetic protein 9 (BMP9) by redox-dependent proteolysis. *J Biol Chem* 2014;289:31150-31159.
10. Long L, Ormiston ML, Yang X, Southwood M, Gräf S, Machado RD, Mueller M, Kinzel B, Yung LM, Wilkinson JM, Moore SD, Drake KM, Aldred MA, Yu PB, Upton PD, Morrell NW. Selective enhancement of endothelial BMPR-II with BMP9 reverses pulmonary arterial hypertension. *NatMed* 2015;21:777-785.
11. Benjamini Y, Hochberg Y. Controlling the false discovery rate - a practical and powerful approach to multiple testing. *J R Stat Soc B* 1995;57:289-300.